Measurement of baryon production in B-meson decay

G. Crawford,[a] R. Fulton,[a] T. Jensen,[a] D. R. Johnson,[a] H. Kagan,[a] R. Kass,[a]
R. Malchow,[a] F. Morrow,[a] J. Whitmore,[a] P. Wilson,[a] D. Bortoletto,[b] D. Brown,[b] J. Dominick,[b]
R. L. McIlwain,[b] D. H. Miller,[b] M. Modesitt,[b] C. R. Ng,[b] S. F. Schaffner,[b] E. I. Shibata,[b] I. P. J. Shipsey,[b]
M. Battle,[c] H. Kroha,[c] K. Sparks,[c] E. H. Thorndike,[c] C.-H. Wang,[c] M. S. Alam,[d] I. J. Kim,[d]
W. C. Li,[d] X. C. Lou,[d] B. Nemati,[d] V. Romero,[d] C. R. Sun,[d] P.-N. Wang,[d] M. M. Zoeller,[d]
M. Goldberg,[e] T. Haupt,[e] N. Horwitz,[e] V. Jain,[e] Rosemary Kennett,[e] M. D. Mestayer,[e] G. C. Moneti,[e]
Y. Rozen,[e] P. Rubin,[e] T. Skwarnicki,[e] S. Stone,[e] M. Thusalidas,[e] W.-M. Yao,[e] G. Zhu,[e]
A. V. Barnes,[f] J. Bartelt,[f] S. E. Csorna,[f] T. Letson,[f] J. Alexander,[g] M. Artuso,[g] C. Bebek,[g]
K. Berkelman,[g] D. Besson,[g] T. Browder,[g] D. G. Cassel,[g] E. Cheu,[g] D. M. Coffman,[g] P. S. Drell,[g]
R. Ehrlich,[g] R. S. Galik,[g] M. Garcia-Sciveres,[g] B. Geiser,[g] B. Gittelman,[g] S. W. Gray,[g] D. L. Hartill,[g]
B. K. Heltsley,[g] K. Honscheid,[g] J. Kandaswamy,[g] N. Katayama,[g] D. L. Kreinick,[g] J. D. Lewis,[g] G. S. Ludwig,[g]
J. Masui,[g] J. Mevissen,[g] N. B. Mistry,[g] S. Nandi,[g] E. Nordberg,[g] C. O'Grady,[g] J. R. Patterson,[g]
D. Peterson,[g] M. Pisharody,[g] D. Riley,[g] M. Sapper,[g] M. Selen,[g] A. Silverman,[g] H. Worden,[g]
M. Worris,[g] A. J. Sadoff,[h] P. Avery,[i] A. Freyberger,[i] J. Rodriguez,[i] J. Yelton,[i] S. Henderson,[j]
K. Kinoshita,[j] F. Pipkin,[j] M. Procario,[j] M. Saulnier,[j] R. Wilson,[j] J. Wolinski,[j] D. Xiao,[j]
Hitoshi Yamamoto,[j] R. Ammar,[k] P. Baringer,[k] D. Coppage,[k] R. Davis,[k] P. Haas,[k] M. Kelly,[k]
N. Kwak,[k] Ha Lam,[k] S. Ro,[k] Y. Kubota,[l] J. K. Nelson,[l] D. Perticone,[l] R. Poling,[l] and
S. Schrenk[l]

[a]*Ohio State University, Columbus, Ohio 43210*
[b]*Purdue University, West Lafayette, Indiana 47907*
[c]*University of Rochester, Rochester, New York 14627*
[d]*State University of New York at Albany, Albany, New York 12222*
[e]*Syracuse University, Syracuse, New York 13244*
[f]*Vanderbilt University, Nashville, Tennessee 37235*
[g]*Cornell University, Ithaca, New York 14853*
[h]*Ithaca College, Ithaca, New York 14850*
[i]*University of Florida, Gainesville, Florida 32611*
[j]*Harvard University, Cambridge, Massachusetts 02138*
[k]*University of Kansas, Lawrence, Kansas 66045*
[l]*University of Minnesota, Minneapolis, Minnesota 55455*

(CLEO Collaboration)

(Received 15 April 1991)

Using the CLEO detector at the Cornell Electron Storage Ring, we observe B-meson decays to Λ_c^+ and report on improved measurements of inclusive branching fractions and momentum spectra of other baryons. For the inclusive decay $\bar{B}\to\Lambda_c^+X$ with $\Lambda_c^+\to pK^-\pi^+$, we find that the product branching fraction $B(\bar{B}\to\Lambda_c^+X)B(\Lambda_c^+\to pK^-\pi^+)=(0.273\pm0.051\pm0.039)\%$. Our measured inclusive branching fractions to noncharmed baryons are $B(B\to pX)=(8.0\pm0.5\pm0.3)\%$, $B(B\to\Lambda X)=(3.8\pm0.4\pm0.6)\%$, and $B(B\to\Xi^-X)=(0.27\pm0.05\pm0.04)\%$. From these rates and studies of baryon-lepton and baryon-antibaryon correlations in B decays, we have estimated the branching fraction $B(\bar{B}\to\Lambda_c^+X)$ to be $(6.4\pm0.8\pm0.8)\%$. Combining these results, we calculate $B(\Lambda_c^+\to pK^-\pi^+)$ to be $(4.3\pm1.0\pm0.8)\%$.

PACS number(s): 13.25.+m, 14.40.Jz

I. INTRODUCTION

Since B mesons can decay into final states with charmed or noncharmed baryons, they offer a unique laboratory for the study of baryon production in weak decays. The noncharmed baryons such as protons, Λ's, and Ξ^-'s may be produced either from the secondary decays of charmed baryons or directly from hadronization processes via virtual W^- or spectator-quark fragmentation. Inclusive decays of B mesons into noncharmed baryons have already been reported by CLEO [1,2] and by ARGUS [3], who have also presented the first direct evidence [4] for B decays to the charmed baryon Λ_c^+. Here, we report on improved measurements of these processes.

In Sec. II, we present the detector description and the particle identification procedures. Section III describes the analysis procedures and reports on measurements of the inclusive branching fractions into various baryons. In Sec. IV, we discuss various possible mechanisms for baryon production in B decays and present results on

baryon-lepton and baryon-antibaryon correlations. In Sec. V, we make first estimates of several absolute branching fractions for B decays into charmed baryons and for the charmed baryon Λ_c^+ decays into baryons. Our conclusions and summary are presented in Sec. VI and an Appendix describes our Monte Carlo model for B-meson decay to baryons, including fits to the various momentum spectra.

II. DATA SAMPLE AND DETECTOR CONSIDERATIONS

This analysis is based on an integrated luminosity of 212 pb^{-1} at the $\Upsilon(4S)$ resonance ($E_{\text{c.m.}}=10.580$ GeV) and 101 pb^{-1} on the continuum at energies just below the threshold for producing $B\bar{B}$ ($\langle E_{\text{c.m.}}\rangle=10.5$ GeV). This corresponds to about 10^6 hadronic events at the resonance, of which 240 000 are $B\bar{B}$ pairs [5] and 760 000 are events from the continuum background under it. The 370 000 hadronic events at the continuum energies are used as subtraction to obtain the $\Upsilon(4S)$ contribution.

The data were collected using the CLEO detector operating at the Cornell Electron Storage Ring (CESR) during 1987–1988. The detector [6] and our hadronic-event selection criteria [7] have been described in detail elsewhere. The tracking system consists of a 51-layer main drift chamber, a 10-layer high resolution drift chamber, and an innermost 3-layer straw tube vertex detector, all within a 1.0-T solenoidal field provided by a coil of radius 1.0 m. The momentum resolution achieved by this system is $(\sigma_p/p)^2=(0.23\%p)^2+(0.7\%)^2$, with p in GeV/c. The dE/dx resolution of the main chamber is 6.5% with a solid angle coverage [8] of 80% of 4π.

Surrounding the magnet coil are other systems to help in particle identification. Plastic scintillators provide time-of-flight (TOF) information with 350 psec resolution over 50% of the solid angle [9]. This timing information is useful for lepton identification and for deriving inclusive proton rates at momenta in excess of 1.0 GeV/c [10]. Outside the scintillators is a lead-proportional tube electromagnetic calorimeter used in electron identification, followed by a steel hadron filter of thickness 0.6 to 1.0 m. Muons are detected by a system of crossed drift chamber planes mounted outside this absorber.

We define a track to be *consistent* with a pion, kaon, or proton hypothesis if its measured dE/dx is within 2σ of its expected value, with σ the rms experimental dE/dx resolution. A charged track is loosely (positively) *identified* as a kaon or proton if, in addition to being consistent with the specific mass hypothesis, the measured dE/dx is at least 1σ (2σ) away from that expected for the pion hypothesis. Similar definitions are made for the TOF measurements on protons for which σ is then the timing resolution.

Proton (antiproton) identification efficiencies as a function of track momenta are found by using kinematically identified protons (antiprotons) from a sample of Λ's ($\bar{\Lambda}$'s), reconstructed as $p\pi^-$ ($\bar{p}\pi^+$) pairs. With 7000 such identifications, the statistical errors on the proton identification efficiencies are about 5% to 10%, depending on momentum. For the antiproton production analysis, the particle identification efficiencies are found separately using a pure sample of antiprotons only and will be discussed later. We use a clean sample of about 900 D^{*+}, detected as $D^0\pi^+$ (with $D^0\to K^-\pi^+$) decays, to measure kaon identification efficiencies for track momenta above 0.5 GeV/c. Kaon identification efficiencies for track momenta below 0.5 GeV/c are obtained using a sample of 7200 ϕ mesons, detected as K^-K^+ pairs over a large combinatorial background. Because of the limited size of the first sample and large background subtractions in the case of the second, the kaon identification efficiencies are known to an accuracy of only 10% to 15%.

To measure the probability that a pion will be misidentified as a kaon or proton, we use pions from a clean sample of about 100 000 K_S^0 mesons, detected in the decay mode $\pi^+\pi^-$. Since we use loose kaon and positive proton identification in our analysis later, we show in Figs. 1(a) and 1(b) the dE/dx identification efficiencies for loosely identified kaons and positively identified protons as a function of track momenta. Also shown in these figures are the corresponding momentum-dependent pion-to-kaon and pion-to-proton misidentification probabilities. The efficiencies and misidentification probabilities are averaged over the two charged states of the particles. Since these are defined for charged tracks already reconstructed in the drift chamber, the effects of the solid angle and reconstruction inefficiencies are not included.

Our lepton identification criteria have been described elsewhere [7]. Briefly, electron identification is achieved using dE/dx measurements in the main drift chamber, the TOF information, and the shower information from the calorimeter. For 47% of the solid angle all three devices contribute, and the electron identification efficiency is 92% with a hadron misidentification probability of 0.3%. For an additional 32% of the solid angle we have only dE/dx measurements; the efficiency in this region is 77%, with misidentification probability of 0.8%. Muons are detected in 72% of the solid angle; the overall efficiency for identifying muons, including the solid angle acceptance, is 60% for momenta above 1.9 GeV/c and falls to 22% at 1.5 GeV/c. The probability of misidentification of a hadron as a muon varies from 0.7% at 1.5 GeV/c to 1.7% above 2.3 GeV/c.

III. INCLUSIVE BARYON PRODUCTION IN B DECAYS

A. $B\to pX$

To measure the inclusive branching fraction [11] $B(B\to pX)$, we use only antiprotons because interactions of particles in the beam pipe produce a large background in the proton sample. Further, a stronger definition of identification is used to select the $\bar{p}$ candidates; the specific ionization (dE/dx) or time-of-flight (TOF) measurement for the track must be within 2σ of the expected value for the antiproton and at least 2σ away from that expected for *both* the pion and kaon, as opposed to posi-

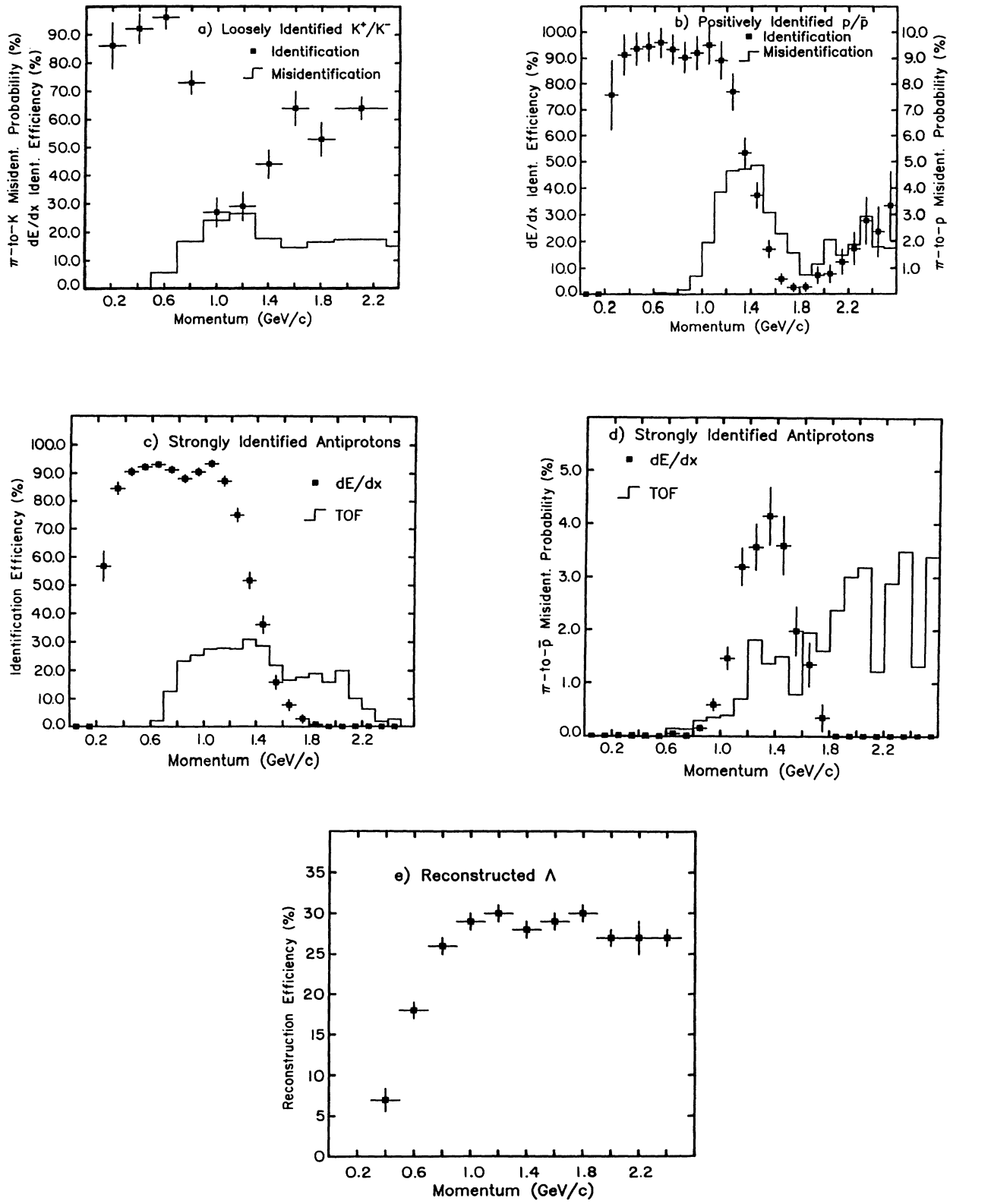

FIG. 1. (a) Identification efficiency and pion-to-kaon misidentification probability for loosely identified kaons using dE/dx, as averaged over K^+ and K^-. (b) Identification efficiency and pion-to-proton misidentification probability for positively identified protons using dE/dx, as averaged over protons and antiprotons. (c) Identification efficiency for strongly identified antiprotons using dE/dx only and TOF only, obtained using clean antiprotons from $\bar{\Lambda}$'s. (d) Pion-to-antiproton misidentification probability for strongly identified antiprotons using dE/dx only and TOF only, obtained using clean pions from K^0_S's. (e) Λ reconstruction efficiency including the branching fraction for $\Lambda \to p\pi^-$.

tive identification, which requires that the dE/dx or TOF measurement for the track be within 2σ of the expected value for the antiproton and at least 2σ away from that expected for the pion only. We include all charged tracks, whether they come from the primary vertex or secondary vertices. No selection cut is applied which would bias against antiprotons produced from $\bar{\Lambda}$'s.

Hadrons produced in B decay at the $\Upsilon(4S)$ are kinematically limited to momenta below 2.5 GeV/c. Furthermore, antiprotons below 0.3 GeV/c suffer large energy losses in the beam pipe and range out or are poorly measured. We therefore determine the number of $\bar{p}$ candidates for the $\Upsilon(4S)$ and for the continuum, limiting the momentum to 0.3 through 2.5 GeV/c. Since we do not *a priori* know the $\bar{p}$ momentum spectrum, we cannot calculate an average efficiency, but must divide the spectrum into a number of smaller momentum bins, performing the analysis in each bin independently.

Even for the strong identification defined above, pions and kaons are occasionally misidentified as antiprotons. To subtract this background, we also measure the number of *positively* identified π^-'s and K^-'s in each momentum interval. The produced numbers of π^-'s, K^-'s, and $\bar{p}$'s are related to the numbers actually observed according to the equation

$$\begin{pmatrix} N_p \\ N_K \\ N_\pi \end{pmatrix} = \mathbf{M}^{-1} \begin{pmatrix} N_p^0 \\ N_K^0 \\ N_\pi^0 \end{pmatrix} . \tag{1}$$

The matrix $\mathbf{M}$ is defined as

$$\mathbf{M} = \begin{pmatrix} \epsilon_p & f_{Kp} & f_{\pi p} \\ f_{pK} & \epsilon_K & f_{\pi K} \\ f_{p\pi} & f_{K\pi} & \epsilon_\pi \end{pmatrix} . \tag{2}$$

The particle indices refer to only negatively charged particles. N_i and N_i^0 are the respective numbers of produced and observed particles of type i. The efficiency for identifying particle type i is ϵ_i and does not include the geometrical acceptance or track reconstruction efficiency of the identifying device. The probability of misidentifying particle type i as j is f_{ij}. Both ϵ_i and f_{ij} are functions of the track momentum. All matrix elements are calculated using clean samples of identified π^-'s, K^-'s and $\bar{p}$'s from the data as discussed above in the hadron identification procedure. Contamination from muons is negligible. Electron contamination is also negligible except for a confusion with $\bar{p}$ in the momentum interval 0.9 to 1.1 GeV/c. In this momentum range the TOF (but not the dE/dx) rejection of electrons is still useful. The matrix is measured for each momentum interval and its inverse matrix calculated using matrix inversion procedures. The matrix is measured using only the dE/dx measurements at low momenta (0.3 to 0.7 GeV/c) and only TOF measurements at higher momenta (0.9 to 1.7 GeV/c). In the momentum region common to both devices (0.7 to 0.9 GeV/c), we use the weighted average of the measurements from the two devices. The consistency of the measurements from the two devices in this momentum region provides confidence in our measurements and is used to estimate the systematic errors.

The track reconstruction efficiency $\epsilon_r(p)$ including the corrections for the solid angle of the detector and absorption in the beam pipe is determined from a Monte Carlo simulation of the detector to be about 85% and 54% for the dE/dx and TOF systems, respectively. For tracks entering the fiducial volumes of the dE/dx and TOF systems, the $\bar{p}$ identification efficiencies and the corresponding π^--to-$\bar{p}$ misidentification probabilities are displayed in Figs. 1(c) and 1(d), respectively.

To find $N_{\bar{p}}$, the number of antiprotons produced in the fiducial volume of a selected device, the analysis has to be carried out for all three particle species simultaneously, and as a function of the particle momentum. In each momentum bin, $N_{\pi^-}^0$, $N_{K^-}^0$, and $N_{\bar{p}}^0$, the raw yields from direct B meson decays, are obtained by subtracting the scaled continuum contribution from that of the $\Upsilon(4S)$ as shown below:

$$N_i^0(p) = [\Delta y_r^B(p)]_i = [y_r^{4S}(p)]_i - f[y_r^{\text{cont}}(p)]_i . \tag{3}$$

The symbol y_r stands for the raw yield in a selected momentum bin and the scale factor $f = 2.08 \pm 0.01$ accounts for the difference in the integrated luminosities and continuum cross sections at the two energies in the data sample. The matrix $\mathbf{M}$ is then determined for each momentum interval as discussed above. From Eq. (1), we obtain the produced yields N_{π^-}, N_{K^-}, and $N_{\bar{p}}$, which still have to be corrected for $\epsilon_r(p)$: $\Delta y_c(p) = N_{\bar{p}}(p)/\epsilon_r(p)$. These corrected $\bar{p}$ yields are then multiplied by 2 to take into account the assumed equal contribution from protons, obtaining the values reported in Table I.

Plotted in Fig. 2 and entered in the last column of Table I are the corrected hadron yields per B decay:

$$\frac{1}{N_B}\frac{dy_c}{dp} = \frac{1}{2N_{B\bar{B}}}\frac{\Delta y_c(p)}{\Delta p} , \tag{4}$$

with $N_{B\bar{B}}$ being the total number of $B\bar{B}$ events and

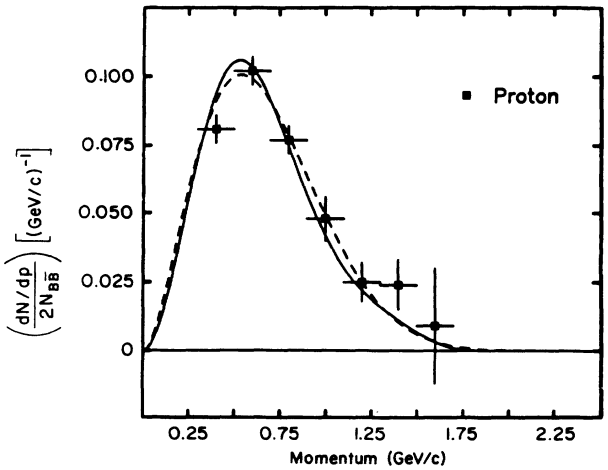

FIG. 2. Momentum spectrum of $\bar{p}$ produced in B decays. The solid curve is a fit to the spectrum using the Monte Carlo model described in the Appendix, while the dashed curve is a fit using the functions described in the text.

TABLE I. Inclusive $\bar{p}$ production in B decays.

Δp (GeV/c)	Yields of $\bar{p}$'s from B decays: Using dE/dx candidates	Using TOF candidates	$2\times\bar{p}$ candidates	$\frac{1}{N_B}\frac{dy_c}{dp}$ [(GeV/c)$^{-1}$]
0.3–0.5	3885±248		7770±496	0.081±0.005
0.5–0.7	4913±249		9826±498	0.102±0.005
0.7–0.9	3620±242	4042±561	7372±444	0.077±0.005
0.9–1.1		2320±366	4640±732	0.048±0.008
1.1–1.3		1190±338	2380±676	0.025±0.007
1.3–1.5		1160±418	2320±836	0.024±0.009
1.5–1.7		455±990	910±1980	0.009±0.021
0.3–1.7			35 218±2511	
	Fitted yield = 38 579±2167±1665			
	$B(B\to pX)=(8.0\pm0.5\pm0.3)\%$			

$N_B = 2N_{B\bar{B}}$. There is no observed $\bar{p}$ signal from B decays beyond 1.7 GeV/c. Summing the contributions from 0.3 to 1.7 GeV/c gives 35 218±2511 p and $\bar{p}$ candidates from B decays.

We now fit this observed spectrum with varying polynomial forms [12], taking the statistical error to be the uncertainty in the fitted area and the systematic uncertainty to be the spread in values for the area from the various functions. This procedure [13] gives a p and $\bar{p}$ yield over the entire momentum range of 38 579±2167±1665, from which we calculate the inclusive branching ratio $B(B\to pX)=(8.0\pm0.5\pm0.3)\%$. The systematic uncertainty is dominated by the uncertainty in the fit to the momentum spectrum and includes a (1 to 3)% error from the $\bar{p}$ identification efficiency. Note that this branching fraction includes those protons coming from intermediate states such as Λ.

B. $\bar{B}\to\Lambda_c^+ X$

We have used the $pK^-\pi^+$ decay mode of the Λ_c^+ to search for the decay $\bar{B}\to\Lambda_c^+ X$. In this and all studies of final states other than $\bar{p}X$ (preceding subsection), we include charge-conjugate states in the sample [11]. All $pK^-\pi^+$ combinations are formed using loosely identified kaon and positively identified proton candidates, with the remaining charged tracks interpreted as pion candidates. The pion candidates are required to have momenta greater than 0.3 GeV/c, which reduces the combinatorial background significantly with only a small loss in Λ_c^+ reconstruction efficiency. Only $pK^-\pi^+$ combinations with momentum less than 2.5 GeV/c are considered; this cutoff is somewhat above the 2.2 GeV/c kinematic limit for Λ_c^+ from B decays. Figure 3 shows the invariant $pK^-\pi^+$ mass distributions for the $\Upsilon(4S)$ and for the scaled continuum data, clearly demonstrating an excess at the resonance. The smooth curve is a fit to the data with a Gaussian signal with a full width at half maximum (FWHM) of 16 MeV/c^2, as predicted by Monte Carlo simulation. The mean from this Gaussian fit is 2284.9±1.5 MeV/c^2, consistent with the Λ_c^+ mass of 2285.0±0.6±1.5 MeV/c^2 obtained from Λ_c^+ continuum production at CLEO [14] and with the current world average [15] of 2285.2±1.2 MeV/c^2.

We have studied the possibility that the observed Λ_c^+ signal is artificially produced from the decays $D^+\to K^-\pi^+\pi^+$ and $D_s^+\to K^-K^+\pi^+$, with either a pion or a kaon misidentified as a proton. The invariant masses of $pK^-\pi^+$ candidates within 2σ of the Λ_c^+ mass have been recalculated with the proton candidate interpreted as a pion or a kaon; we see no evidence for an enhancement in the region of the D^+ or D_s^+ mass.

In each momentum bin we determine the raw yields for the continuum $y_r^{\rm cont}(p)$ and resonance data $y_r^{4S}(p)$ by fitting the observed $pK^-\pi^+$ invariant mass spectrum to a Gaussian with the experimental mean of 2284.9 MeV/c^2 and a width determined from Monte Carlo simulation for Λ_c^+ baryons of that momentum. These raw yields, the

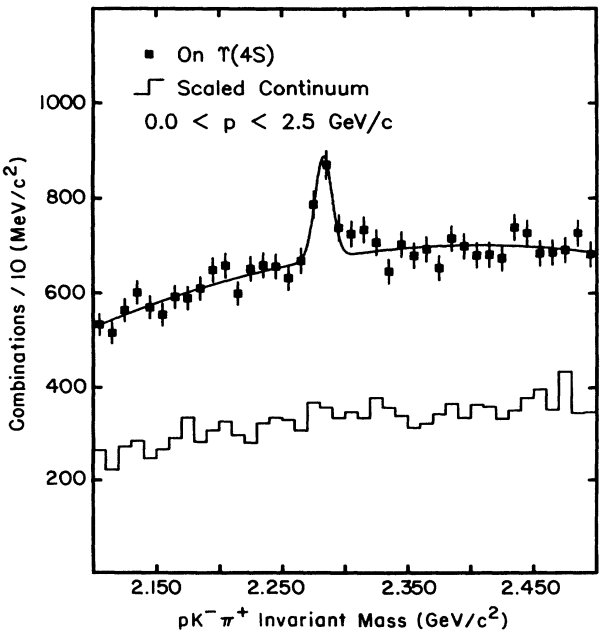

FIG. 3. $pK^-\pi^+$ invariant-mass distributions from $\Upsilon(4S)$ and scaled continuum for $p<2.5$ GeV/c.

reconstruction efficiencies $\epsilon_r(p)$, and the corrected yields $\Delta y_c(p)$ are presented in Table II, while the spectrum itself is displayed in Fig. 4. Since the exclusive branching fractions of the Λ_c^+ are not well known, our plotted momentum distribution necessarily contains the factor $B(\Lambda_c^+ \to pK^-\pi^+)$. Fitting this spectrum [12], we find $1310\pm247\pm188$ Λ_c^+ baryons produced in B decays and detected in the $pK^-\pi^+$ decay mode, from which we extract the product branching fraction $B(B \to \Lambda_c^+ X) \times B(\Lambda_c^+ \to pK^-\pi^+) = (0.273\pm0.051\pm0.039)\%$. The systematic error is dominated by a 12% uncertainty in the Λ_c^+ reconstruction efficiency, including the uncertainties in kaon and proton identification, and an 8% uncertainty in the raw yields due to the fitting and background subtraction procedure. The systematic uncertainty introduced by the fitting of the Λ_c^+ momentum spectrum is less than 2%.

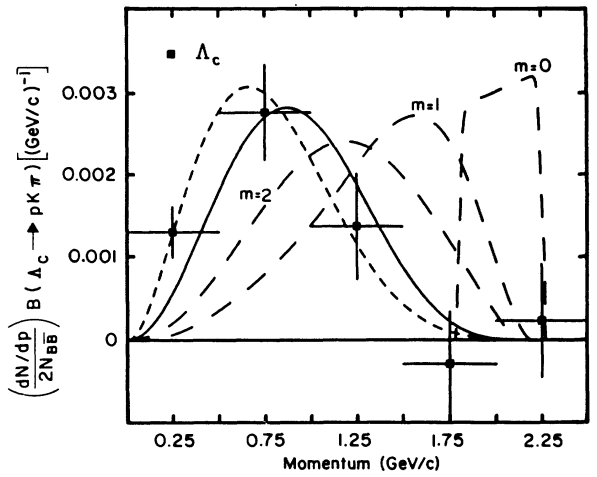

FIG. 4. Momentum spectrum for Λ_c^+ produced in $\bar{B}$ decays. The solid curve is derived from the Monte Carlo model described in the Appendix which has $\bar{B} \to \Lambda_c^+ \bar{N} X$. The short dashed curve is a fit using the functions described in the text. The three long dashed curves are from a model in which X is explicitly $(m\pi)$, with m labeled on each curve. For $m=0$, the area under the curve is scaled by $\frac{1}{2}$.

C. $B \to \Lambda X$

Using the $p\pi^-$ decay mode of the Λ, we have measured $B(B \to \Lambda X)$ [11]. Λ candidates are formed from pairs of oppositely charged tracks which intersect at a radial distance of more than 1 mm from the primary vertex. The dE/dx measurements of the positive tracks had to be *consistent* with those expected for protons. At low Λ momentum the reconstruction efficiency $\epsilon_r(p)$ becomes very small, so only $p\pi^-$ combinations with momentum 0.3 to 2.5 GeV/c are considered. This efficiency, which includes the branching fraction $B(\Lambda \to p\pi^-)$ [15], varies from 5% to 30% over this momentum region as displayed in Fig. 1(e) and tabulated in Table III.

Figure 5 displays the invariant-mass spectra for the $\Upsilon(4S)$ and scaled continuum data for all $p\pi^-$ combinations which satisfy the above selection criteria, indicating an excess of events associated with direct B decays. According to the Monte Carlo simulation, the experimental mass resolution varies from 8 MeV/c^2 at low momentum (dominated by multiple scattering) to 3 MeV/c^2 at higher momentum. The fit shown to the $\Upsilon(4S)$ distribution is the sum of a first order polynomial background and three Gaussian functions with widths (FWHM) equal to 3, 5, and 8 MeV/c^2. The means of the three Gaussians are consistent with each other and within 1.4 MeV/c^2 of the established mass [15] of 1115.63 MeV/c^2, indicating the degree to which we understand energy loss in the beam pipe and detector walls. The total number of Λ's from B decays is found according to the momentum-dependent analysis procedure described earlier and presented in detail in Table III. This table also shows that the raw Λ yield from B decays in the momentum region 2.5 to 2.9 GeV/c is consistent with being zero, indicating that the continuum subtraction has been carried out correctly. The measured momentum spectrum of Λ's from B decays is plotted in Fig. 6.

The total corrected yield of Λ from B decays in the momentum region 0.3 to 2.5 GeV/c is $15\,949\pm1830$, with the error being statistical only. Fitting this spectrum as described previously [12], we find $18\,142\pm1734\pm2873$ Λ's produced [13], for an inclusive branching fraction $B(B \to \Lambda X) = (3.8\pm0.4\pm0.6)\%$. The second error is systematic, dominated by contributions of 14% from the fitting of the momentum spectrum, 7% from the Λ yields from the fitting procedure, and 5% from the Λ recon-

TABLE II. Inclusive Λ_c^+ production in B decays.

Δp	Raw $\Lambda_c^+/\overline{\Lambda_c^+}$ yields			$\epsilon_{\Lambda_c^+}(p)$	Corr. yield	$(1/N_B)(dy_c/dp)$
(GeV/c)	$y_r^{4S}(p)$	$fy_r^{\rm cont}(p)$	$\Delta y_r^B(p)$	(%)	$\Delta y_c(p)$	$[(\text{GeV}/c)^{-1}]$
0.0–0.5	62±14	−10±9	72±17	23	313±74	0.0013±0.0003
0.5–1.0	154±26	−5±21	159±33	24	663±138	0.0028±0.0006
1.0–1.5	86±27	7±25	79±37	24	329±154	0.0014±0.0006
1.5–2.0	13±20	27±23	−14±30	20	−70±150	−0.0003±0.0006
2.0–2.5	52±16	43±20	9±26	16	56±163	0.0002±0.0007
0.0–2.5	367±48	62±46	305±66	24	1291±312	

Fitted yield = 1310±247±188

$B(\bar{B} \to \Lambda_c^+ X) B(\Lambda_c^+ \to pK^-\pi^+) = (0.273\pm0.051\pm0.039)\%$

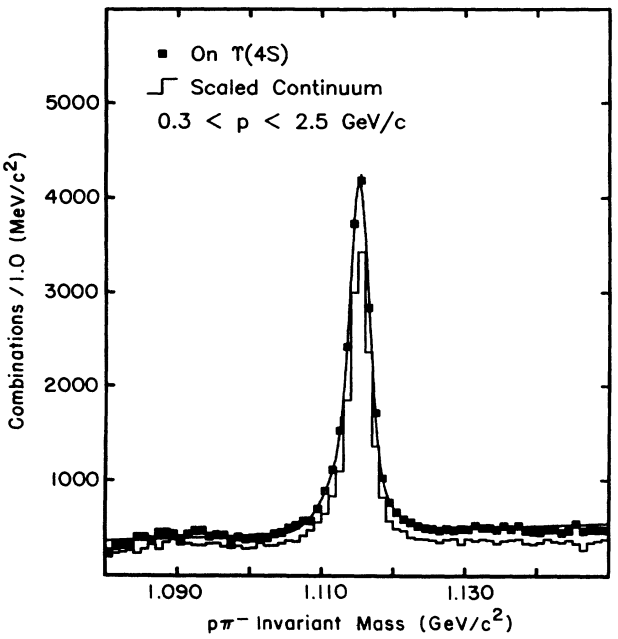

FIG. 5. $p\pi^-$ invariant-mass distributions from $\Upsilon(4S)$ and scaled continuum for $0.3 < p < 2.5$ GeV/c.

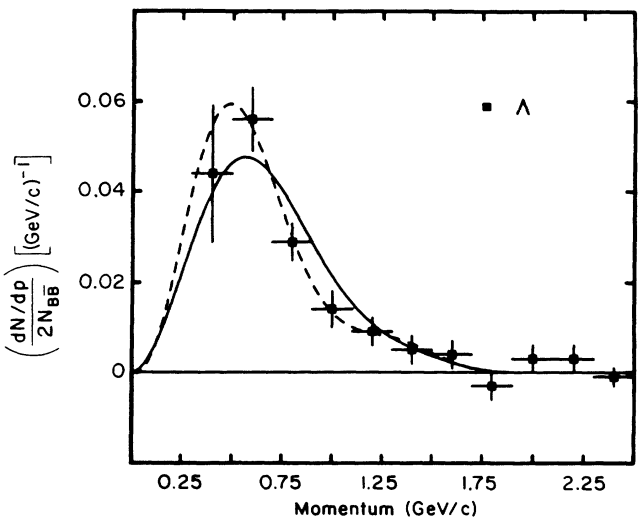

FIG. 6. Momentum spectrum of Λ baryons produced in B decays. The solid curve is a fit to the spectrum using the Monte Carlo model described in the Appendix, while the dashed curve is a fit using the functions described in the text.

struction efficiencies. This quoted branching fraction includes Λ's that have higher-mass baryons as parents and we have assumed the Λ's are unpolarized.

D. $B \to \Xi^- X$

The inclusive branching fraction [11] $B(B \to \Xi^- X)$ is measured through the decay chain $\Xi^- \to \Lambda\pi^-$ and $\Lambda \to p\pi^-$. The Λ candidates are selected as described in Sec. III C. We then consider combinations of Λ with additional negatively charged tracks in the event such that the vertex of the Ξ^- candidate be at least 4 mm away from the primary vertex and closer to it than the Λ vertex. Further, since the contribution of Ξ^-'s produced from continuum e^+e^- annihilations is large, we require that the Fox-Wolfram [16] shape parameter R_2 be less than 0.5. This shape requirement eliminates 60% of the continuum events and is more than 99.5% efficient for events from B decays in this channel. The systematic uncertainty associated with this cut is found to be much smaller than other systematic sources and we therefore neglect this contribution in the determination of the overall systematic error. The Ξ^- reconstruction efficiency $\epsilon_r(p)$, which includes the branching fractions into the observed final state, varies from 8% at 0.25

TABLE III. Inclusive Λ production in B decays.

Δp (GeV/c)	Raw $\Lambda/\bar{\Lambda}$ yields $y_r^{4S}(p)$	$f y_r^{\rm cont}(p)$	$\Delta y_r^B(p)$	$\epsilon_\Lambda(p)$ (%)	Corr. Yield $\Delta y_c(p)$	$(1/N_B)(dy_c/dp)$ $[(\text{GeV}/c)^{-1}]$
0.3–0.5	1200±60	902±81	298±101	7	4257±1443	0.044±0.015
0.5–0.7	2749±74	1776±91	973±117	18	5406±650	0.056±0.007
0.7–0.9	2782±63	2050±77	732±99	26	2815±381	0.029±0.004
0.9–1.1	2412±56	2013±84	399±101	29	1376±348	0.014±0.004
1.1–1.3	2099±58	1841±76	258±96	30	860±320	0.009±0.003
1.3–1.5	1687±55	1550±69	137±88	28	489±314	0.005±0.003
1.5–1.7	1281±52	1157±66	124±84	29	428±290	0.004±0.003
1.7–1.9	1122±57	1212±78	−90±97	30	−300±323	−0.003±0.003
1.9–2.1	882±48	792±61	90±78	27	333±289	0.003±0.003
2.1–2.3	730±41	640±54	90±68	27	333±252	0.003±0.003
2.3–2.5	425±28	438±46	−13±54	27	−48±200	−0.001±0.002
2.5–2.7	308±26	376±56	−68±62			
2.7–2.9	244±25	204±40	40±47			
0.3–2.5	17 369±182	14 371±240	2998±302	19	15 949±1830	
Fitted yield = 18 142±1734±2873						
$B(B \to \Lambda X) = (3.8 \pm 0.4 \pm 0.6)\%$						

GeV/c to 13% above 1.5 GeV/c (see Table IV). Figure 7 shows the resulting invariant-mass distribution for $\Lambda\pi^-$ combinations with momenta less than 2.5 GeV/c from the $\Upsilon(4S)$ and scaled continuum data samples. Again, an excess of baryons associated with B decays is evident. The smooth curve is a fit to the $\Upsilon(4S)$ distribution with the width of the Gaussian fixed at 6.5 MeV/c^2, as determined by Monte Carlo simulation. For the Ξ^- this width is essentially independent of momentum. From this fit the mass is 1321.0±0.3 MeV/c^2 to be compared with the world average value [15] of 1321.32±0.13 MeV/c^2. The raw and corrected yields are determined as described previously and detailed in Table IV, with the momentum spectrum itself displayed in Fig. 8.

Fitting the momentum spectrum [12] below 2.5 GeV/c, we find 1304±228±190 Ξ^-'s from B decays, from which we calculate $B(B\to\Xi^- X)=(0.27\pm0.05\pm0.04)\%$. The systematic error is dominated by a 10% uncertainty in the Ξ^- reconstruction efficiency and a 10% uncertainty in the fitting procedure which gives the raw yields. The fitting of the Ξ^- momentum spectrum has an associated systematic uncertainty of only 4%.

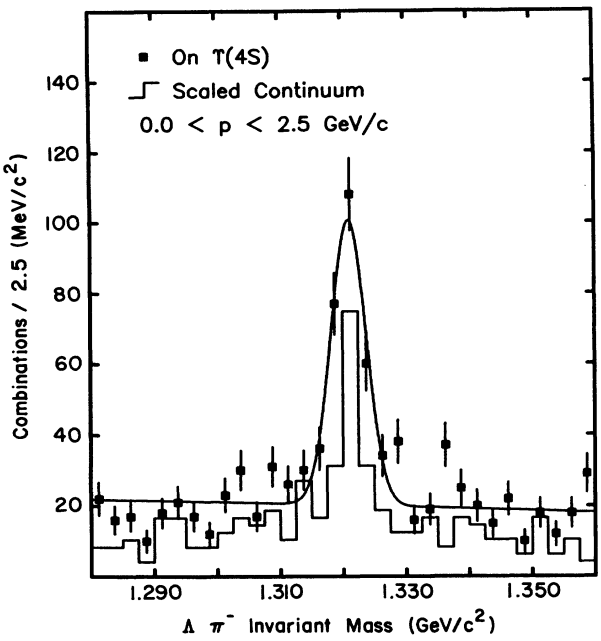

FIG. 7. $\Lambda\pi^-$ invariant-mass distributions from $\Upsilon(4S)$ and scaled continuum for $p<2.5$ GeV/c.

IV. DETERMINATION OF BARYON PRODUCTION MECHANISMS

A. Enumeration of possible mechanisms

There are many possible mechanisms for baryon production in B-meson decay; they depend on the b-quark coupling ($b\to cW^-$, $b\to uW^-$, or $b\to sg$) and the type of diagram (spectator, exchange, annihilation, or penguin). To conserve baryon number, the final state must always contain a baryon-antibaryon pair, limiting the number of diagrams. To describe these final states in generic terms, let N stand for baryons with $S=C=0$ (p,n,Δ, and N^*), Y be for those with $S=-1, C=0$ (Λ, Σ^0, Σ^+, and Σ^-), Ξ denote $S=-2, C=0$ baryons (Ξ^- and Ξ^0), Y_c represent those with $S=0, C=1$ (such as Λ_c^+, Σ_c^0, Σ_c^+, and Σ_c^{++}), and Ξ_c symbolize those with $S=-1, C=1$ (Ξ_c^0 and Ξ_c^+). In the meson sector, D is a generic $S=0, C=1$ particle (D^0 and D^+), and D_s^- is an $S=-1, C=1$ particle. X is any combination of charmless mesons, with or without leptons. We have not considered final states which require popping of at least two $s\bar{s}$ pairs from the vacuum sea, since these must be doubly suppressed.

(a) $Y_c\bar{N}X, \Xi_c\bar{Y}X$. These final states are produced from $b\to cW^-$ coupling through either spectator or exchange diagrams, as shown in Fig. 9(a). We expect the $\Xi_c\bar{Y}X$ states to be suppressed with respect to $Y_c\bar{N}X$ states since they require the popping of an $s\bar{s}$ pair from the vacuum sea.

(b) $DN\bar{N}X, DY\bar{Y}X$. In the left of Fig. 9(b), the charmless baryon-antibaryon pair is produced by fragmentation at the W^- vertex and the D meson is formed from the charm and spectator quark. This final state can also be produced from the right diagram in the same figure. There is no *a priori* reason that these mechanisms should be suppressed.

(c) $\Xi_c\bar{Y}_cX$ and $\bar{Y}_cYX$. These states are produced through the color-mixed spectator diagram with $W^-\to\bar{c}s$. Contributions from these states are small compared to those from final states of type (a) since $B(b\to c\bar{c}s)/B(b\to\text{all})$ is estimated to be roughly 15–19 % [17,18]. Decays to $\Xi_c\bar{Y}_cX$ are also suppressed

TABLE IV. Inclusive Ξ^- production in B decays.

Δp (GeV/c)	Raw $\Xi^-/\overline{\Xi^-}$ yields $y_r^{4S}(p)$	$fy_r^{\text{cont}}(p)$	$\Delta y_r^B(p)$	$\epsilon_\Xi(p)$ (%)	Corr. yield $\Delta y_c(p)$	$(1/N_B)(dy_c/dp)$ [(GeV/c)$^{-1}$]
0.0–0.5	17±5	7±7	10±9	8	125±113	0.0005±0.0005
0.5–1.0	85±10	17±9	68±13	10	680±130	0.0028±0.0005
1.0–1.5	78±10	33±11	45±15	12	375±125	0.0016±0.0005
1.5–2.0	36±7	16±8	20±11	13	154±85	0.0006±0.0004
2.0–2.5	6±4	2±6	4±7	13	31±54	0.0001±0.0002
0.0–2.5	222±17	75±19	147±25	11	1365±235	
			Fitted yield $=1304\pm228\pm190$			
			$B(B\to\Xi^- X)=(0.27\pm0.05\pm0.04)\%$			

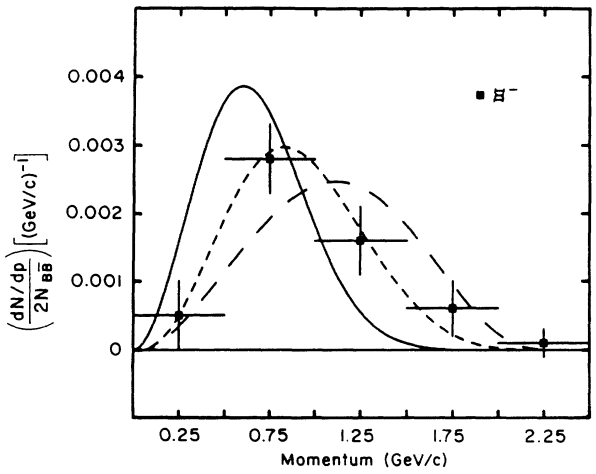

FIG. 8. Momentum spectrum for Ξ^- produced in $\bar{B}$ decays. The solid curve represents the prediction from the Monte Carlo model as described in the Appendix with $\bar{B}\to\Lambda_c^+\bar{N}X$ and $\Lambda_c^+\to\Xi^-K^+\pi^+$. The short dashed curve is a fit using the functions described in the text. Further we show with a long dashed curve the prediction from the model $\bar{B}\to\Xi_c^0\bar{\Sigma}X$ with $\Xi_c^0\to\Xi^-\pi^+$. If instead we let $\Xi_c^0\to\Xi^-X$ or $\Xi_c^0\to\Xi^-\pi^+\pi^0$ the curves are essentially the same as the short dashed functional fit.

by phase space since both Ξ_c and Y_c are each over 2 GeV/c^2 in mass. The decays to $\bar{Y}_c YX$ are further suppressed since the coupling is $b\to uW^-$ and $|V_{bu}/V_{bc}|\approx 0.1$ [19,20]. There is also some possible suppression in both decays due to the color mixing, but this is not well understood.

(d) $D_s^- Y_c\bar{N}X$ and $D_s^-\Xi_c\bar{Y}X$. This is the same as (a) but with $W^-\to\bar{c}s$; hence it should be suppressed with respect to (a).

(e) $Y\bar{N}X$. Decays of this type can only be produced from the $b\to sg$ coupling through penguin diagrams. CLEO has shown that contributions to B decay from various exclusive penguin diagrams are negligible [21].

(f) $N\bar{N}X$, $Y\bar{Y}X$. These are states without charm and are

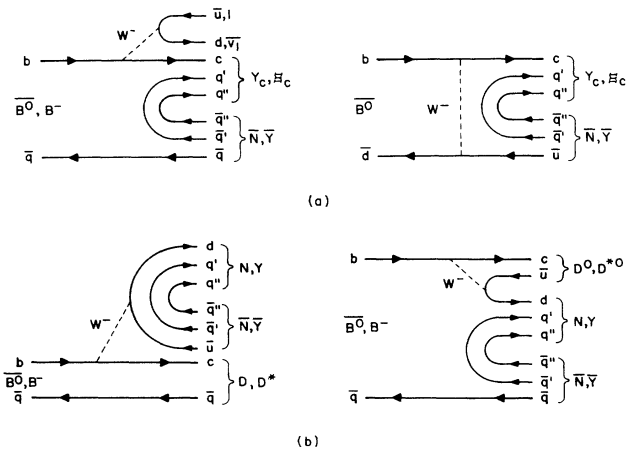

FIG. 9. Prominent decay diagrams for B decays to baryons. Shown are final states of the form (a) $Y_c\bar{N}X$ and $\Xi_c\bar{Y}X$, and (b) $DN\bar{N}X$ and $DY\bar{Y}X$.

produced from the $b\to uW^-$ coupling through either the spectator, exchange, or annihilation diagram. We expect contributions from decays of this type to be small because of the suppression of the $b\to uW^-$ relative to $b\to cW^-$ coupling.

One way to discriminate among the various decays is to look for particle-particle correlations in events. We have investigated four such correlations: $\Lambda\bar{\Lambda}$, Λ-lepton, $\Lambda\bar{p}$, and $p\bar{p}$. These analyses are described below.

B. Study of $\Lambda\bar{\Lambda}$ correlations

B decays to baryons should therefore be dominated by the final states $Y_c\bar{N}X$, $DN\bar{N}X$, $\Xi_c\bar{Y}X$, and $DY\bar{Y}X$ (see Fig. 9). Only the last two of these four can result in the final state $\Lambda\bar{\Lambda}X$; study of $\Lambda\bar{\Lambda}$ correlations can therefore discriminate between these production mechanisms. If decays of the type $\Lambda\bar{\Lambda}X$ were the source of all Λ's in B decay, the ratio $f_{\Lambda\bar{\Lambda}}=B(B\to\Lambda\bar{\Lambda}X)/B(B\to\Lambda X)$ would be 0.5. Values of $f_{\Lambda\bar{\Lambda}}$ near this maximal value would mean the decays $\Xi_c\bar{Y}X$ and $DY\bar{Y}X$ are dominant. Small values of $f_{\Lambda\bar{\Lambda}}$ come about if the decays $Y_c\bar{N}X$ and $DN\bar{N}X$ are dominant or if large number of hyperons materialize as Σ^+ or Σ^-, since these do not decay to Λ [22].

We have thus searched for $\Lambda\bar{\Lambda}X$ final states. A $\Lambda(\bar{\Lambda})$ candidate is defined as a pair of oppositely charged tracks forming a secondary vertex satisfying the selection procedure defined in Sec. III C except that the Λ mass selection cut is not applied at this point. Only candidates with momenta between 0.4 and 2.3 GeV/c are included, the upper cut being near the kinematic limit for Λ's produced from $B\to\Lambda\bar{\Lambda}X$. Figure 10 is the scatter plot of the masses of the Λ and $\bar{\Lambda}$ candidates from the same event for all $\Upsilon(4S)$ and continuum data. We select $\Lambda\bar{\Lambda}$ candidate events by requiring

$$\sqrt{\Delta M_\Lambda^2+\Delta M_{\bar{\Lambda}}^2}\le 6\ \text{MeV}/c^2\ , \tag{5}$$

where 6 MeV/c^2 is the width of the Λ signal in the $p\pi^-$ mass distribution. The selected regions are shown as solid circles. We estimate the background under the signal regions by considering the average of similar circular sidebands on all sides of the signal region marked as dashed circles in the figure. After subtracting backgrounds, we find 332 ± 22 and 132 ± 13 $\Lambda\bar{\Lambda}$ events on the $\Upsilon(4S)$ and continuum, respectively. Subtracting the scaled continuum contribution, we get for $N_{\Lambda\bar{\Lambda}X}$, the contribution from direct $\Upsilon(4S)$ decays,

$$N_{\Lambda\bar{\Lambda}X}=57\pm35\ . \tag{6}$$

We still have to subtract $n_{\Lambda\bar{\Lambda}X}$, the contribution for the case where Λ and $\bar{\Lambda}$ candidates are produced from different B's. This can be calculated from the equation

$$n_{\Lambda\bar{\Lambda}X}=N_{B\bar{B}}\epsilon_\Lambda^2[B(\bar{B}\to\bar{\Lambda}_{\text{only}}X)\times B(B\to\Lambda_{\text{only}}X) + B(\bar{B}\to\Lambda_{\text{only}}X)\times B(B\to\bar{\Lambda}_{\text{only}}X)]\ , \tag{7}$$

where ϵ_Λ is the product of the Λ reconstruction efficiency and the acceptance for the lower-momentum cut, and has been found from a Monte Carlo simulation to be

$(15\pm1)\%$. Further, we use the measured branching fraction [11] from Table III:

$$B(\bar{B}\to\Lambda X)=B(\bar{B}\to\Lambda_{\text{only}}X)+B(\bar{B}\to\bar{\Lambda}_{\text{only}}X)$$
$$=(3.8\pm0.4\pm0.6)\% \ . \tag{8}$$

If we assume $B(\bar{B}\to\bar{\Lambda}_{\text{only}}X)=B(B\to\Lambda_{\text{only}}X)=0$, we get $n_{\Lambda\bar{\Lambda}X}=8\pm3$; alternatively, if we assume the very unlikely case $B(\bar{B}\to\Lambda_{\text{only}}X)=B(\bar{B}\to\bar{\Lambda}_{\text{only}}X)$, we get $n_{\Lambda\bar{\Lambda}X}=4\pm2$. To be conservative and encompass both of these possibilities, we use 6.5 ± 4.5 as this contribution.

The contribution from $B\to\Lambda\bar{\Lambda}X$ is then

$$N_{B\to\Lambda\bar{\Lambda}X}=(N_{\Lambda\bar{\Lambda}X}-n_{\Lambda\bar{\Lambda}X})/\epsilon_{\Lambda\bar{\Lambda}} \ . \tag{9}$$

The reconstruction efficiency for $\Lambda\bar{\Lambda}X$ produced in $B\bar{B}$ decays, $\epsilon_{\Lambda\bar{\Lambda}}$, is found to be $(4.0\pm0.4)\%$ based on a Monte Carlo model with equal mixtures of $B\to D\Lambda\bar{\Lambda}$, $B\to D\Lambda\bar{\Lambda}\pi$, and $B\to D^*\Lambda\bar{\Lambda}$ decay modes. We finally obtain

$$N_{B\to\Lambda\bar{\Lambda}X}=1263\pm891 \ . \tag{10}$$

This corresponds to an inclusive branching fraction [11]

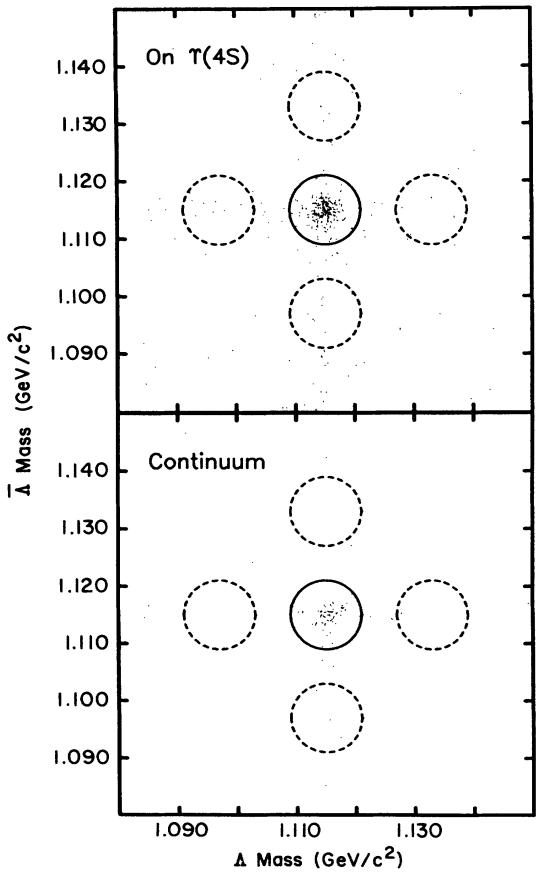

FIG. 10. Masses of Λ and $\bar{\Lambda}$ candidates from the same event for all $\Upsilon(4S)$ and continuum data. The continuous circles mark the regions for selecting $\Lambda\bar{\Lambda}$ candidates (signal region), whereas the dashed circles show the regions used for background estimation.

$B(B\to\Lambda\bar{\Lambda}X)<0.50\%$ and ratio $f_{\Lambda\bar{\Lambda}}<13\%$, both at the 90% C.L. This result suggests that it is unlikely that the final states $\Xi_c\bar{Y}X$ and $DY\bar{Y}X$ are dominant in B decay.

C. Study of Λ-lepton correlations

Measuring Λ-lepton correlations in B decays can help determine whether final states of the type $Y_c\bar{N}X$ [such as in Fig. 9(a)] or those of the type $DY\bar{Y}X$ [as in Fig. 9(b)] are dominant in Λ formation. Studying these correlations therefore complements our study of $\Lambda\bar{\Lambda}$ correlations described above. Using the notation of Sec. IV A, with the additional definition of X_h as one or more *hadrons*, we can enumerate the different possible sources of Λ-lepton correlations. The two processes of interest, from which we get a high-momentum muon or electron with which to tag the B flavor, are (i) $\bar{B}\to Y_c\bar{N}X_h$, $Y_c\to\Lambda X_h$, $B\to X_h l^+\nu$, (ii) $\bar{B}\to\Lambda\bar{\Lambda}X_h$, $B\to X_h l^+\nu$.

There are other processes which produce leptons of lower momentum, that can be considered backgrounds in our study:

(iii) $\bar{B}\to Y_c\bar{N}X_h$, $Y_c\to\Lambda l^+\nu$, $B\to$hadrons ,

(iv) $\bar{B}\to Y_c\bar{N}l^-\bar{\nu}$, $Y_c\to\Lambda X_h$, $B\to$hadrons ,

(v) $\bar{B}\to Y_c\bar{N}X_h$, $Y_c\to\Lambda X_h$, $B\to D_iX_h$, $D_i\to X_h l^-\bar{\nu}$, where $D_i=\overline{D^0}$, D^-, or D_s^- ,

(vi) $\bar{B}\to Y_c\bar{N}X_h$, $Y_c\to\Lambda X_h$, $B\to\bar{Y}_cNX_h$, $\bar{Y}_c\to\bar{\Lambda}l^-\bar{\nu}$.

Finally, we will also need to consider correlations observed due to ψ (ψ') production and due to misidentification of hadrons as leptons:

(vii) $\bar{B}\to Y_c\bar{N}X_h$, $Y_c\to\Lambda X_h$, $B\to\psi X_h$, $\psi\to l^+l^-$.

(viii) $\bar{B}\to\Lambda X_h$ or $\bar{\Lambda}X_h$; $B\to$hadrons, hadrons misidentified as leptons .

Processes (i) and (iii) contribute only to Λl^+ correlations, (iv) and (v) contribute only to Λl^- correlations, and (ii), (vi), (vii), and (viii) contribute to both the correlations. After accounting for the contributions from processes (iii) to (viii) and correcting for the effects of $B^0\overline{B^0}$ mixing, the observation of Λl^+ and absence of Λl^- correlations would point towards the importance of $Y_c\bar{N}X$ as the dominant mechanism for B decay to Λ. Therefore, we refer to the Λl^+ as the right sign (R) and Λl^- as the wrong sign (W) correlations. Equal rates for the two correlations would support the process $DY\bar{Y}X$ as the dominant mechanism.

To search for Λ-lepton candidate events, we consider electrons and muons with momenta between 1.4 and 2.4 GeV/c and Λ candidates with momenta between 0.4 and 2.0 GeV/c. The criteria for the identification of electron, muon, and Λ candidates have been discussed in Secs. II and III. The lower lepton momentum cut suppresses leptons from the secondary decays of charmed particles, as will be discussed below. The upper Λ and lepton momenta cuts correspond to the upper limit of the corresponding observed momentum spectra in B decays. Another

effective way to suppress the background is to require $-0.8 < \cos\theta_{\Lambda l} < 0.9$, where $\theta_{\Lambda l}$ is the angle between the Λ and the lepton in the laboratory frame. For continuum processes, the $\cos\theta_{\Lambda l}$ distribution tends to be peaked in the forward and backward directions. For Λ and leptons produced from different B's, no angular correlation is expected and hence this distribution is expected to be flat. The angular correlation cut removes about 75% of the continuum contribution at the expense of only 15% of that from B decay. Figure 11 shows the $p\pi^-$ invariant-mass distributions for events with Λl^+ (R) and Λl^- (W) candidates after continuum subtraction. Fitting the data with the mass and width found from the inclusive Λ sample, we obtain 112 ± 12 Λl^+ and 41 ± 8 Λl^- candidates. Before we can draw any conclusions about the baryon production mechanism, we must first subtract from these results the contributions from the other background physics processes enumerated above and correct for $B^0\overline{B^0}$ mixing.

We have used data and Monte Carlo simulations to estimate the contributions to the measured correlations signal from all the processes listed above. In the momentum range 0.4 to 2.0 GeV/c, we have measured a raw yield of $N_\Lambda^{\rm obs}=2543\pm274$ Λ's or $\overline{\Lambda}$'s from B-meson decays. This sample includes contributions from 51 ± 35 events in which both the Λ and $\overline{\Lambda}$ are detected in the same event, and is referred to as $\Lambda\overline{\Lambda}$ events (see Sec. IV B). It is clear that in most of the events above the Λ ($\overline{\Lambda}$) is coming from a $\overline{B}$ (B), so that we can estimate the correlation contributions from the opposite B ($\overline{B}$) meson by simulating its semileptonic decay according to available data. The contribution from the $\Lambda\overline{\Lambda}$ events to either sign correlations is negligible. It should be noted that the contributions from all the background processes will be calculated without making any assumptions about the final states of which the Λ's are secondary products, except in the case of process (iv), in which some model-dependent assumptions cannot be avoided.

In Fig. 12, we show the Monte Carlo generated lepton spectra from processes (i) and (ii), and the background processes (iii) to (vi). These plots do not include the effect of smearing of the track momenta. However, while calculating the acceptance corresponding to the different momentum selection criteria, a Monte Carlo simulation of the tracks in the drift chambers is used. The spectra from the background processes are peaked at low momenta with most of the distribution below 1.4 GeV/c, which is why we chose this value as our cutoff. With this selection criterion, processes (iii) and (vi) do not contribute at all since 1.4 GeV/c is beyond the kinematic limit for leptons from these processes. This also eliminates events in which the initial lepton is a τ which subsequently decays to a lighter lepton.

For the processes in category (v), the general form of the correlation contribution may be written as

$$N_{\Lambda l^-}=N_\Lambda^{\rm obs}B(B\to D_iX_h)B(D_i\to X_hl^-\nu)\alpha_l\ , \qquad (11)$$

where $\alpha_l=\epsilon_p\epsilon_\theta\epsilon_l$, and D_i denotes $\overline{D^0}$, D^-, or D_s^-. The latest values of the branching fractions [15] are used in the calculations. The factor $\epsilon_p\approx0.05\pm0.01$ is the acceptance corresponding to the momentum selection criteria $1.4<p_l<2.4$, while $\epsilon_\theta=0.85\pm0.05$ is the acceptance for the selection cut $-0.8<\cos\theta_{\Lambda l}<0.9$. They are approximately the same for the different D_i. These acceptance factors are estimated by generating $B\to D_iX$ according to the measured D_i spectrum from B-meson decays and then allowing $D_i\to Xl^-\bar{\nu}$, again matching the l^- momentum spectrum to the measured shape [23]. The factor ϵ_l is the momentum-dependent lepton detection efficiency. It is different for electrons and muons and includes the effect of the solid angle of the devices. For electrons,

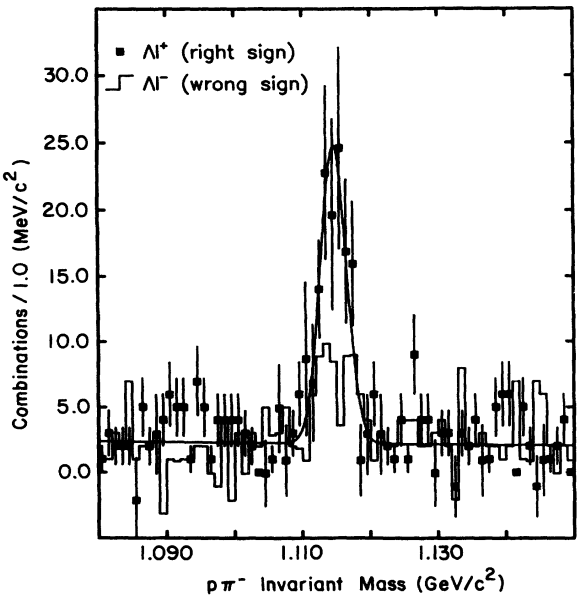

FIG. 11. $p\pi^-$ invariant-mass distributions for Λl^+ (R) and Λl^- (W) candidates from B decays, obtained after continuum subtraction.

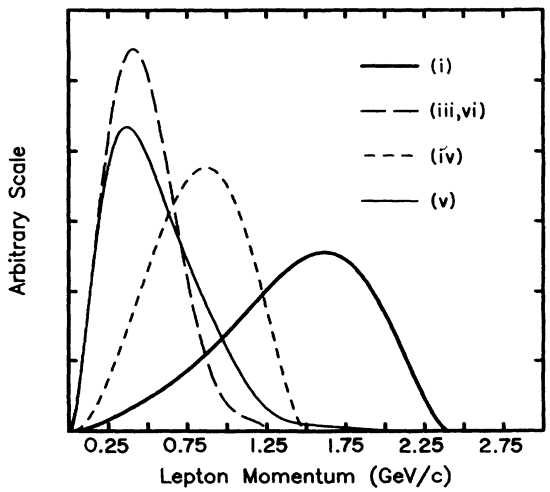

FIG. 12. Expected lepton momentum spectra for the reactions (i) and (ii) $B\to X_hl^+\nu$; (iii) $\overline{B}\to\Lambda_c^+\overline{N}X_h$, $\Lambda_c^+\to\Lambda l^+\nu$; (iv) $\overline{B}\to\Lambda_c^+\overline{N}l^-\bar{\nu}$, $\Lambda_c^+\to\Lambda X_h$; (v) $B\to\overline{D}X_h$, $\overline{D}\to X_hl^-\bar{\nu}$ with $\overline{D}=\overline{D^0}, D^-, D_S^-$; (vi) $B\to\overline{\Lambda_c^+}NX_h$, $\overline{\Lambda_c^+}\to\overline{\Lambda}l^-\bar{\nu}$.

$\epsilon_e = 0.59 \pm 0.04$ and nearly independent of momentum. For muons ϵ_μ, averaged over the relevant momentum range, is 0.35 ± 0.04. It should be noted that for processes in this category $N_{\Lambda l^+} = 0$. When calculating the contributions from these background processes, we have not included the effect of mixing, which would change the result by less than 1 event.

The contributions from process (vii) are calculated in a similar way, except, in this case, $N_{\Lambda l^-} = N_{\Lambda l^+}$, and the overall acceptance factor $\alpha_e = 0.45 \pm 0.10$ and $\alpha_\mu = 0.27 \pm 0.06$.

Process (iv) contributes only to the wrong sign correlations. This contribution can be written as

$$N_{\Lambda l^-} = N_{B\bar{B}} B(\bar{B} \to Y_c \bar{N} l^- \bar{\nu}) B(Y_c \to \Lambda X) \alpha_\Lambda \alpha_l \ , \tag{12}$$

where α_Λ and α_l are the overall Λ and l^- acceptance factors, respectively, as defined earlier. In Eq. (12), $B(\bar{B} \to Y_c \bar{N} l^- \bar{\nu})$ and $B(Y_c \to \Lambda X)$ are both unknown. Multiplying the right-hand side by $B(\bar{B} \to Y_c X)/B(\bar{B} \to Y_c X) = 1$ and assuming that all Λ are produced from Y_c, i.e., $N_\Lambda^{\rm obs} = N_{B\bar{B}} B(\bar{B} \to Y_c X) B(Y_c \to \Lambda X) \alpha_\Lambda$, yields

$$N_{\Lambda l^-} = N_\Lambda^{\rm obs} \frac{B(\bar{B} \to Y_c \bar{N} l^- \bar{\nu})}{B(\bar{B} \to Y_c X)} \alpha_l \ . \tag{13}$$

If any $\Lambda\bar{\Lambda}$ type of final state would be the source of Λ, then the number of wrong sign correlations from process (iv) would be lowered. We have inflated the systematic errors on $N_{\Lambda l^-}$ to reflect this uncertainty in the procedure. We now assume that

$$\frac{B(\bar{B} \to Y_c \bar{N} l^- \bar{\nu})}{B(\bar{B} \to Y_c X)} = \frac{B(\bar{B} \to X l^- \bar{\nu})}{B(\bar{B} \to \text{all})} = B_{\rm SL} \ , \tag{14}$$

which is just the measured semileptonic branching fraction for B mesons. The factor α_l is found by simulating process (iv) using the Monte Carlo simulation developed later in the paper, which reproduces the shape of the measured Λ and Λ_c^+ momentum spectrum. It should be noted that the Monte Carlo simulation is used only to estimate the fraction of leptons which pass the momentum and angular selection criteria and knowledge of the unmeasured branching fractions mentioned above is not required. We obtain $\alpha_e = 0.015 \pm 0.006$ and $\alpha_\mu = 0.005 \pm 0.002$.

The contribution from hadrons faking leptons, process (viii), is calculated using the measured hadron spectrum from events containing an identified Λ or $\bar{\Lambda}$ and the measured misidentification probabilities, also calculated from the data as discussed earlier in Sec. II. Since we should have an approximately equal number of positively and negatively charged hadrons, we expect the faking hadrons to contribute equally to both correlations. This contribution can be calculated as

$$N_{\Lambda l^-} = \sum_{p_i = 1.4}^{2.4\ \text{GeV}/c} \{ N_{\rm neg}^\Lambda(p_i) [f_{e^-}(p_i) + f_{\mu^-}(p_i)] + N_{\rm pos}^{\bar{\Lambda}}(p_i) [f_{e^+}(p_i) + f_{\mu^+}(p_i)] \} \ , \tag{15}$$

where $N_{\rm neg}^\Lambda(p_i)$ and $N_{\rm pos}^{\bar{\Lambda}}(p_i)$ are the number of negatively and positively charged hadron tracks found in events with a Λ or $\bar{\Lambda}$, respectively, in the momentum interval centered at p_i. The corresponding probabilities for hadrons to fake electrons or muons are given by f_{e^-} and f_{μ^-}, respectively. We have measured faking probabilities by averaging over negatively and positively charged tracks, and over different hadron species. The hadron-to-electron faking probability is $(0.6 \pm 0.1)\%$ and nearly independent of momentum, while the hadron-to-muon faking probability varies from $(0.6 \pm 0.1)\%$ at 1.4 GeV/c to $(1.7 \pm 0.3)\%$ at 2.4 GeV/c.

The phenomenon of $B^0\bar{B}^0$ mixing has been observed by both ARGUS [24] and CLEO [25]. The mixing parameter $r = (N_{B^0B^0} + N_{\bar{B}^0\bar{B}^0})/N_{B^0\bar{B}^0}$ has been measured to be 0.21 ± 0.08 and 0.165 ± 0.065, respectively. When a $B^0\bar{B}^0$ transforms to a B^0B^0 or $\bar{B}^0\bar{B}^0$ event, an expected Λl^+ correlation transforms to a Λl^- correlation. The loss of Λl^+ correlations turns up as a gain in Λl^- correlations. The contribution from $B^0\bar{B}^0$ mixing is calculated assuming the $\Upsilon(4S)$ decays to neutral $B\bar{B}$ pairs 50% of the time [26]. The number of mixed events relative to the total before mixing is given by

$$\frac{N_{B^0B^0} + N_{\bar{B}^0\bar{B}^0}}{N_{B^0\bar{B}^0} + (N_{B^0B^0} + N_{\bar{B}^0\bar{B}^0})} = \frac{r}{1+r} = 0.142 \pm 0.056 \ , \tag{16}$$

where we have used only the CLEO number to be self-consistent.

The loss of right sign Λl^+ correlations from the events before mixing may be calculated using

$$\Delta N^{R \to W} = 0.5 N_\Lambda^{\rm obs} \frac{r}{1+r} B(B \to X l^+ \nu) \alpha_l \ . \tag{17}$$

Thus this number should be added to Λl^+ and subtracted from the Λl^- observed correlations.

The accounting for the processes (iii) to (viii) are listed in Table V. After subtracting the contribution from these background processes and correcting for the effect of $B^0\bar{B}^0$ mixing, we observe 112 ± 13 Λl^+ and 9 ± 10 Λl^- correlations candidates, which must be due to processes (i) and (ii). We note that the observed Λl^- signal is consistent with zero [27].

Below we calculate the expected correlation signals from the measured yield of $N_\Lambda^{\rm obs} = 2543 \pm 274$ Λ or $\bar{\Lambda}$ and $N_{\Lambda\bar{\Lambda}}^{\rm obs} = 51 \pm 35$ $\Lambda\bar{\Lambda}$ events:

$$N_{\Lambda l^+} = N_\Lambda^{\rm obs} B(B \to X l^+ \nu) \alpha_l \ . \tag{18}$$

The factor α_l is found using a Monte Carlo simulation to generate the decay $B \to X l^+ \nu$ according to the measured shape of the lepton spectrum from B-meson decays and the measured lepton detection efficiencies as discussed earlier. We obtain $\alpha_e = 0.25 \pm 0.04$ and $\alpha_\mu = 0.17 \pm 0.02$, from which we calculate an expected 125 ± 19 Λl^+ correlations signal, which is consistent with what we have observed.

For the final states of the form $\bar{B} \to \Lambda\bar{\Lambda}X$, the contribution is equal for right and wrong sign correlations. The right sign correlations contribution is already included in

TABLE V. Summary of Λ-lepton correlations and background calculations.

Source:	Λl^+ correlations		Λl^- correlations	
Processes:	Electrons	Muons	Electrons	Muons
Observed signal (i)–(viii):	112±12		41±8	
Calculations for (iii)–(viii)				
(iii) $\bar{B}\to Y_c\bar{N}X_h, Y_c\to\Lambda l^+\nu; B\to$hadrons	Below p cut			
(iv) $\bar{B}\to Y_c\bar{N}l^-\bar{\nu}, Y_c\to\Lambda X_h; B\to$hadrons			4.7±2.7	1.5±0.9
(v a) $\bar{B}\to Y_c\bar{N}X_h, Y_c\to\Lambda X_h; B\to\bar{D}^0X_h$			1.9±0.7	1.1±0.4
(v b) $\bar{B}\to Y_c\bar{N}X_h, Y_c\to\Lambda X_h; B\to D^-X_h$			2.1±1.0	1.3±0.6
(v c) $\bar{B}\to Y_c\bar{N}X_h, Y_c\to\Lambda X_h; B\to D_s^-X_h$			0.6±0.2	0.4±0.2
(vi) $\bar{B}\to Y_c\bar{N}X_h, Y_c\to\Lambda X_h; B\to\bar{Y}_cX_h$, $\bar{Y}_c\to X_hl^-\bar{\nu}$			Below p cut	
(vii) $\bar{B}\to Y_c\bar{N}X_h, Y_c\to\Lambda X_h; \bar{B}\to\psi X_h$, $\psi\to l^+l^-$	0.9±0.3	0.5±0.2	0.9±0.3	0.5±0.2
(viii) Hadrons faking leptons	7.6±1.4		8.2±1.7	
Background: sum of (iii)→(viii)	9.0±1.4		23.2±3.6	
Correlation signal: obs.–bgnd.	103.0±12.1		17.8±8.8	
$B^0\bar{B}^0$ mixing correction:	9.3±3.8		−(9.3±3.8)	
Final measured correlation signal:	112.3±12.7		8.5±9.6	
Expected correlation signal:	124.6±19.2		2.5±1.3	

the above calculation. Here we calculate the wrong sign correlations contribution:

$$N_{\bar{\Lambda}l^+}=N_{\Lambda\bar{\Lambda}}^{\rm obs}B(B\to Xl^+\nu)\alpha_l\ . \tag{19}$$

The sum of the electron and muon wrong sign contributions is 3±1, which is again consistent with observation.

The absence of $\Lambda\bar{\Lambda}$ and Λl^- correlations and the observation of Λl^+ correlations suggests that intermediate states of the form $Y_c\bar{N}X$ are the dominant source of all Λ's observed in B-meson decays.

D. Study of $\Lambda\bar{p}$ correlations

In the preceding two subsections we have shown that B decays to baryons dominantly proceed via final states $Y_c\bar{N}X$ or $DN\bar{N}X$ and that all Λ in B decay have Y_c parentage. As noted earlier, these conclusions depend on the assumption that there is not an unusually large amount of Σ hyperon production in B decay. If we further assume that Λ_c^+ saturates Y_c then B decays resulting in Λ proceed via the decay $\Lambda_c^+\bar{N}X$. Looking at $\Lambda\bar{p}$ correlations it is then possible to estimate the fraction of the time the $\bar{N}$ is a $\bar{p}$. The relative fractions f_p and f_n, with $f_p+f_n=1$, are defined below:

$$f_p=B(B\to\Lambda_c^+\bar{p}X)/B(B\to\Lambda_c^+X)\ , \tag{20}$$

$$f_n=B(B\to\Lambda_c^+\bar{n}X)/B(B\to\Lambda_c^+X)\ . \tag{21}$$

Under our assumption that all correlations between Λ and $\bar{p}$ observed in B decays are produced from decays of the type $\Lambda_c^+\bar{p}X$, we can write

$$N_\Lambda=N_BB(B\to\Lambda_c^+X)B(\Lambda_c^+\to\Lambda X)\ , \tag{22}$$

$$N_{\Lambda\bar{p}}=N_BB(B\to\Lambda_c^+\bar{p}X)B(\Lambda_c^+\to\Lambda X)\ , \tag{23}$$

where $N_{\Lambda\bar{p}}$ and N_Λ are the total number of $\Lambda\bar{p}$ and Λ candidates produced in N_B decays. Dividing, we obtain

$$\frac{N_{\Lambda\bar{p}}}{N_\Lambda}=\frac{B(B\to\Lambda_c^+\bar{p}X)}{B(B\to\Lambda_c^+X)}=f_p\ . \tag{24}$$

But since we assume every Λ in B decay has a Λ_c^+ parent this ratio can also be expressed as

$$f_p=\frac{N_{\Lambda\bar{p}}}{N_\Lambda}=\frac{B(B\to\Lambda\bar{p}X)}{B(B\to\Lambda X)}\ , \tag{25}$$

making it possible for us to measure f_p from the study of $\Lambda\bar{p}$ correlations in our data.

To search for $\Lambda\bar{p}$ candidates, we use Λ's with momenta between 0.4 and 2.0 GeV/c and strongly identified [28] $\bar{p}$'s with momenta from 0.3 to 1.1 GeV/c. The upper $\bar{p}$ momentum cut reduces contributions from pions being misidentified as $\bar{p}$'s. After continuum subtraction, we observe 1526±121 $\Lambda\bar{p}$ and 190±68 Λp candidates [29]. We may get $\Lambda\bar{p}$ candidates from negative pions or kaons faking antiprotons or when the Λ and $\bar{p}$ are produced from opposite B and $\bar{B}$. Both these sources are equally likely to contribute to $\Lambda\bar{p}$ and Λp candidates, so that we may use the observed Λp signal as an estimate of the background for the $\Lambda\bar{p}$ signal. Thus we observe 1336±139 $\bar{B}\to\Lambda\bar{p}X$ correlations corresponding to 2825±304 $B\to\Lambda X$ candidates with Λ's in the selected momentum range. Correcting for the antiproton identification efficiency which averages about (92±5)% over the selected momentum range, drift chamber track reconstruction efficiency, and solid angle acceptance factor of (85±5)%, and a momentum acceptance correction factor of (80±5)%, we get 2136±222±217 corrected $\Lambda\bar{p}$ candidates. The momentum acceptance correction factor is obtained using the Monte Carlo model for B decays to baryons developed in the Appendix. We do not correct for the Λ detection efficiency since this cancels out in the numerator and the denominator. Thus we calculate $f_p=(76\pm11\pm8)\%$. The second error is systematic and is obtained from the errors in the antiproton-associated

correction factors. Referencing Fig. 9, we note that if charged and neutral B mesons were equally produced, and if only the spectator diagram contributed, then we would expect f_p to be one-half; our measured value is within two standard deviations of that value. We also calculate the inclusive branching fraction $B(B\to\Lambda\bar{p}X)=(2.9\pm0.5\pm0.5)\%$.

E. Study of $p\bar{p}$ correlations

Proton-antiproton correlations arise from protons produced from secondary decays of Λ_c^+ and antiprotons produced in association with them (i.e., via $\Lambda_c^+\bar{p}X$) or from direct decays to $p\bar{p}X$ and $\Lambda\bar{\Lambda}X$. We define $B_{p\bar{p}}=B(B\to p\bar{p}X)$. For this analysis, we use positively identified protons and antiprotons with a momentum between 0.3 and 0.9 GeV/c. To minimize backgrounds from interactions in the beam pipe we impose additional criteria on the vertex of the proton; such a cut is not necessary on the antiprotons. The efficiency of this cut is $\epsilon_{vx}=0.80\pm0.02$. The momentum cut on the protons and antiprotons is tighter than for the case of the $\Lambda\bar{p}$ study since we have a large background from pion and kaon fakes. We expect pions and kaons faking protons and antiprotons to contribute equally to $p\bar{p}$ and pp or $\bar{p}\bar{p}$ correlations. Thus we use the observed pp and $\bar{p}\bar{p}$ signal as an estimate of the background from the pion and kaon fakes as well as that from random pairings, produced in the simultaneous decays of the B and $\bar{B}$ to baryons. After continuum and background subtractions, we obtain 2792 ± 161 $p\bar{p}$ candidates from B decay. To obtain the corrected yield of $p\bar{p}$ candidates, we divide by $\epsilon_{vx}(\epsilon_{id}\epsilon_{dr}\epsilon_p)^2$. Here $\epsilon_{id}=0.92\pm0.02$ is the particle identification efficiency, which is nearly constant over the selected momentum range; $\epsilon_{dr}=0.85\pm0.05$ is the track reconstruction efficiency and the drift chamber solid angle acceptance; and $\epsilon_p=0.70\pm0.04$ is the momentum acceptance corresponding to the model discussed in the Appendix. We thus get $11\,647\pm672\pm1990$ as the total number of $p\bar{p}$ candidates produced, from which we calculate

$$B_{p\bar{p}}=B(B\to p\bar{p}X)=(2.4\pm0.1\pm0.4)\% , \tag{26}$$

where the second error is systematic and reflects the contributions from the errors in the correction factors mentioned above. Note that this branching fraction includes p and $\bar{p}$ from intermediate states such as Λ. We also calculate $f_{p\bar{p}}=B(B\to p\bar{p}X)/B(B\to pX)=(30\pm2\pm5)\%$, where we have used our measured value of $B(B\to pX)$ reported in Table I.

F. Study of $DN\bar{N}$ correlations

We have also searched for B decays to $DN\bar{N}X$ by looking for D^{*+} candidates in our sample of $p\bar{p}$ events. For this aspect of the analysis we imposed an R_2 cut at 0.3 to help eliminate continuum processes. The D^{*+} candidates are found through the decay $D^0\pi^+$ with $D^0\to K^-\pi^+$; the efficiency for detecting such a D^{*+} in B decay, including geometric, tracking, shape parameter, and identification effects, is roughly 18%. We observe three such events in the $\Upsilon(4S)$ sample, all of which have a $D^{*+}p\bar{p}$ invariant mass consistent with coming from a B. There is one such event in the continuum data sample, so the most probable mean of continuum contamination in the $\Upsilon(4S)$ sample is 2.1 events. Since $B(B\to D^{*+}X)=(25\pm3\pm4)\%$ [30], $B(D^{*+}\to D^0\pi^+)=(57\pm4\pm4)\%$ [31], and $B(D^0\to K^-\pi^+)=(4.2\pm0.4\pm0.4)\%$ [31], we expect to observe 2.7 ± 1.0 $D^{*+}p\bar{p}X$ events from cases in which one B decays to $p\bar{p}X$ and the other to $D^{*+}X$. The most probable mean for the level of backgrounds in the $\Upsilon(4S)$ sample is therefore 4.8 events. Consistent with observation, we conclude there are no $D^{*+}p\bar{p}X$ events from B decay and use 2.3 events to obtain an upper limit on this process [32]. Given the 25% efficiency for finding the $p\bar{p}$ (see discussion on $p\bar{p}$ correlations), we set a 90%-C.L. limit of $B(B\to D^{*+}p\bar{p}X)<0.4\%$. Taking the production of vector mesons to be twice that of pseudoscalars [26,30] and assuming equal population of the four $N\bar{N}$ combinations [33] then yields the corresponding limit, again at 90% confidence,

$$B(B\to DN\bar{N}X)<4.8\% . \tag{27}$$

Given our result $B(B\to pX)=8.0\%$ (from Sec. III A) and previous results [2,3] that have shown baryon production to account for roughly 10% of all B decay, we will assume $DN\bar{N}X$ is not dominant in our analysis.

V. ESTIMATION OF ABSOLUTE BRANCHING FRACTIONS

Building on our measured branching fractions and our observed correlations we can, with some reasonable assumptions, estimate or set limits on many interesting absolute branching fractions, in particular $B(\Lambda_c^+\to pK^-\pi^+)$. The study of $\Lambda\bar{\Lambda}$ correlations shows that the forms $Y_c\bar{N}X$ and $DN\bar{N}X$ are the main contributors to B decays to baryons, with $\Xi_c\bar{Y}X$ and $DY\bar{Y}X$ being weaker sources (see Fig. 9); this observation is valid unless there is an unusually large production of Σ hyperons in B decay. Our Λ-lepton correlation study indicates that in B decay all Λ baryons, a natural source of final state p and n, come from Y_c parentage. A negative search for B decays to $D^{*+}p\bar{p}X$ indicates that $DN\bar{N}X$ is also not a dominant decay mechanism.

A. Results assuming dominance of Λ_c^+X

We now assume that *all* baryons in B decay come from $Y_c\bar{N}X$ (i.e., that $DN\bar{N}X$ and $\Xi_c\bar{Y}X$ are heavily suppressed) and that Λ_c^+ saturates Y_c. These assumptions are supported by our Monte Carlo model, which assumes $\Lambda_c^+\bar{N}X$ as the only source of baryons, simultaneously fitting the momentum spectra for p, Λ_c^+, and Λ as shown in Figs. 2, 4, and 6 (see Appendix). Later we will use our observation of Ξ^- to estimate the actual amount of $\Xi_c\bar{Y}X$ and will indicate how that influences the values of the branching fractions we have derived.

First we define some simplifying notations for B decays [11,34]:

$$B_\alpha=B(B\to\alpha X),\quad \alpha=p,n,\Lambda,\Xi , \tag{28}$$

$$B_{\Lambda_c^+}=B(\bar{B}\to\Lambda_c^+X) . \tag{29}$$

These final-state baryons include contributions from secondary decays of higher-mass baryons. With this notation, the fractions f_p and f_n (see Sec. IV D) are defined by

$$B_{\Lambda_c^+} f_p = B(\bar{B} \to \Lambda_c^+ \bar{p} X) , \tag{30}$$

$$B_{\Lambda_c^+} f_n = B(\bar{B} \to \Lambda_c^+ \bar{n} X) , \tag{31}$$

with, as before, $f_p + f_n = 1$.

Following the decay model assumptions, $\bar{p}$ are produced in association with Λ_c^+'s from decays of the form $\bar{B} \to \Lambda_c^+ \bar{p} X$; protons are produced from the secondary decays of the Λ_c^+'s. This can be expressed as

$$B_p = B_{\Lambda_c^+} f_p + B_{\Lambda_c^+} B(\Lambda_c^+ \to pX) . \tag{32}$$

Proton-antiproton correlations arise when $\bar{B} \to \Lambda_c^+ \bar{p} X$ and $\Lambda_c^+ \to pX$ so that

$$B_{p\bar{p}} = B_{\Lambda_c^+} f_p B(\Lambda_c^+ \to pX) . \tag{33}$$

In Eqs. (32) and (33) we have already determined B_p (Sec. III A), f_p (Sec. IV D), and $B_{p\bar{p}}$ (Sec. IV E), leaving two unknowns. Eliminating $B(\Lambda_c^+ \to pX)$ gives

$$\begin{aligned} B_{\Lambda_c^+} &= (B_p f_p - B_{p\bar{p}})/f_p^2 \\ &= (6.4 \pm 0.8 \pm 0.8)\% , \end{aligned} \tag{34}$$

with the first error being statistical and the latter systematic. This is consistent with the theoretical estimate $B(B \to \Lambda_c^+ \bar{N} X) \approx (2-13)\%$ calculated by Bigi [35] in the context of a simple-minded spectator model for B decays. From Table II, we have

$$B_{\Lambda_c^+} B(\Lambda_c^+ \to pK^- \pi^+) = (0.273 \pm 0.051 \pm 0.039)\% . \tag{35}$$

We thus estimate the *exclusive* branching fraction

$$B(\Lambda_c^+ \to pK^- \pi^+) = (4.3 \pm 1.0 \pm 0.8)\% . \tag{36}$$

Our measurement of $B(\Lambda_c^+ \to pK^- \pi^+)$ is consistent with the value $(4.1 \pm 2.4)\%$ reported by the ARGUS Collaboration [4], using the same procedure as ours. Both results are also consistent with the lower limit of 2.7% (90% C.L.) reported by the Lexan Bubble Chamber–European Hybrid Spectrometer (LEBC-EHS) Collaboration [36]. The new result is higher than the value of $(2.2 \pm 1.0)\%$ reported by the Mark II Collaboration [37], which was also a model dependent estimate of the branching fraction. Any level of $DN\bar{N}X$ or $\Xi_c \bar{Y} X$ in B decay will necessarily *lower* our value for $B_{\Lambda_c^+}$ and *raise* our estimate of $B(\Lambda_c^+ \to pK^- \pi^+)$.

If instead we eliminate $B_{\Lambda_c^+}$ in Eqs. (32) and (33), we obtain an expression for the inclusive branching fraction of Λ_c^+ to protons as

$$\begin{aligned} B(\Lambda_c^+ \to pX) &= \frac{B_{p\bar{p}} f_p}{B_p f_p - B_{p\bar{p}}} \\ &= (50 \pm 8 \pm 14)\% . \end{aligned} \tag{37}$$

The inclusive branching fraction to n follows from the fact that all Λ_c^+ must eventually decay to either p or n:

$$B(\Lambda_c^+ \to nX) = (50 \pm 8 \pm 14)\% . \tag{38}$$

Using these same decay assumptions, the only way to have a Λ in B decay is for $\Lambda_c^+ \to \Lambda X$; i.e., $B_\Lambda = B_{\Lambda_c^+} B(\Lambda_c^+ \to \Lambda X)$. Using the value of $B_{\Lambda_c^+}$ we have just derived and our measured value of B_Λ (Sec. III C), we obtain

$$B(\Lambda_c^+ \to \Lambda X) = (59 \pm 10 \pm 12)\% . \tag{39}$$

Applying our assumptions to inclusive B decays to neutrons gives an expression for B_n similar to that of B_p:

$$\begin{aligned} B_n &= B_{\Lambda_c^+} f_n + B_{\Lambda_c^+} B(\Lambda_c^+ \to nX) \\ &= B_{\Lambda_c^+} [1 - f_p + B(\Lambda_c^+ \to nX)] \\ &= (4.7 \pm 1.1 \pm 1.2)\% , \end{aligned} \tag{40}$$

where we have used our measured value of f_p and our above estimate for the inclusive branching fraction of Λ_c^+ to neutrons.

B. Incorporation of $\Xi_c \bar{Y} X$ in B decays

We expect the decay $\bar{B} \to \Xi_c X$ [38] to be suppressed relative to $\bar{B} \to \Lambda_c^+ X$, since the former can only proceed through $s\bar{s}$ creation from the vacuum sea. Based on reasonable assumptions, it is possible to estimate from our data the value of the relative ratio

$$R_{\Xi_c} = B(\bar{B} \to \Xi_c X)/B(\bar{B} \to \Lambda_c^+ X) . \tag{41}$$

If we assume that all Ξ^- and Ξ^0 have Ξ_c parentage and that all Λ's are produced from Λ_c^+, from Ξ_c via an intermediate Ξ^- or Ξ^0, or in association with a Ξ_c [see Fig. 9(a)], we can write

$$\begin{aligned} N_\Lambda = {} & N_{\Lambda_c^+} B(\Lambda_c^+ \to \Lambda X) \\ & + N_{\Xi_c} B(\Xi_c \to \Xi^- X) B(\Xi^- \to \Lambda X) \\ & + N_{\Xi_c} B(\Xi_c \to \Xi^0 X) B(\Xi^0 \to \Lambda X) \\ & + N_{\Xi_c} \eta , \end{aligned} \tag{42}$$

with η being the fraction of all $\bar{Y}$ that materialize as $\bar{\Lambda}$. If the hyperons are equally probable in production, then $\eta = 0.5$; if $\bar{\Lambda}$ dominates, then η tends toward unity.

The decay rate of Ξ^- and Ξ^0 to Λ's is nearly 100% [15]. For lack of better information, we assume $B(\Xi_c \to \Xi^- X) = B(\Xi_c \to \Xi^0 X)$, making the second and third terms in Eq. (42) equal and reducing it to

$$N_\Lambda = N_{\Lambda_c^+} B(\Lambda_c^+ \to \Lambda X) + N_{\Xi_c} [2B(\Xi_c \to \Xi^- X) + \eta] , \tag{43}$$

which can be rearranged to present the ratio of interest as

$$R_{\Xi_c}=\frac{N_{\Xi_c}}{N_{\Lambda_c^+}}=\frac{N_{\Xi_c}B(\Lambda_c^+\to\Lambda X)}{N_\Lambda-N_{\Xi_c}[2B(\Xi_c\to\Xi^-X)+\eta]}\ . \tag{44}$$

But our assumption about all Ξ^- having Ξ_c parentage can be written as $N_{\Xi^-}=N_{\Xi_c}B(\Xi_c\to\Xi^-X)$ so that the ratio can instead be expressed as

$$R_{\Xi_c}=\frac{N_{\Xi^-}}{N_\Lambda-2N_{\Xi^-}-N_{\Xi_c}\eta}\frac{B(\Lambda_c^+\to\Lambda X)}{B(\Xi_c\to\Xi^-X)}\ . \tag{45}$$

The decay $\Lambda_c^+\to\Lambda X$ is similar to the decay $\Xi_c\to\Xi^-X$. However, the Ξ_c may decay to Ξ^- or Ξ^0. Thus, we may assume that the ratio $\alpha=B(\Lambda_c^+\to\Lambda X)/B(\Xi_c\to\Xi^-X)$ is of the order of 2.0. In the denominator N_{Ξ_c} is simply $R_{\Xi_c}N_{\Lambda_c^+}$. Using branching fractions instead of yields we then have

$$R_{\Xi_c}=\frac{\alpha B_{\Xi^-}}{B_\Lambda-2B_{\Xi^-}-R_{\Xi_c}B^c_{\Lambda_c^+}\eta}\ . \tag{46}$$

The branching fraction $B^c_{\Lambda_c^+}$ differs from our value of $B_{\Lambda_c^+}$ derived in the preceding section because we are now explicitly assuming the existence of $\Xi_c\bar{Y}X$ final states. We can approximate [39]

$$B^c_{\Lambda_c^+}=\frac{B_{\Lambda_c^+}}{1+R_{\Xi_c}}\ . \tag{47}$$

The equation for R_{Ξ_c} is then the quadratic

$$R^2_{\Xi_c}[B_\Lambda-2B_\Xi-\eta B_{\Lambda_c^+}]+R_{\Xi_c}[B_\Lambda-(2+\alpha)B_\Xi]-\alpha B_\Xi=0\ . \tag{48}$$

Values of R_{Ξ_c} are shown as contours in Fig. 13 as a function of α and η. Taking probable values of $\alpha=2.0$ and $\eta=0.75$ and using $B_\Lambda=(3.8\pm0.7)\%$, $B_\Xi=(0.27\pm0.06)\%$, and $B_{\Lambda_c^+}=(6.4\pm1.1)\%$ gives $R_{\Xi_c}=0.25\pm0.12$. Here the statistical and systematic uncertainties have been added in quadrature.

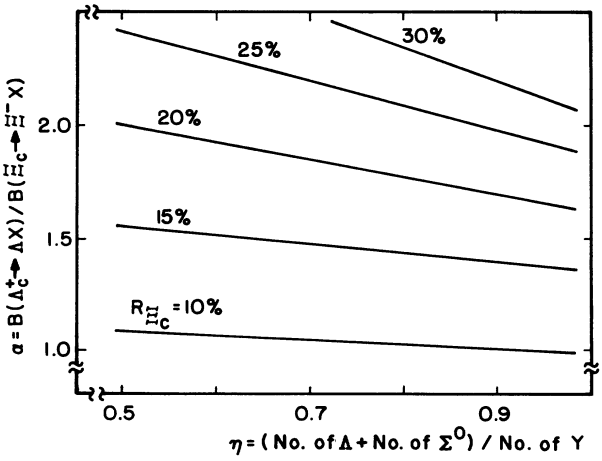

FIG. 13. The value of R_{Ξ_c}, which is the ratio of Ξ_c to Λ_c^+ in B decay, from our data as a function of the unknowns α (which should have a value near 2.0) and η (which is likely to be between 0.5 and 1.0).

This value of R_{Ξ_c} leads to the following corrected values for branching fractions derived in the preceding section, all with large uncertainties:

$$B^c_{\Lambda_c^+}=(5.1\pm1.0)\%\ , \tag{49}$$

$$B^c(\Lambda_c^+\to pK^-\pi^+)=(5.5\pm1.7)\%\ , \tag{50}$$

$$B^c(\Lambda_c^+\to\Lambda X)=(45\pm15)\%\ . \tag{51}$$

We can also use this result for R_{Ξ_c} to make further statements about the relative contributions to B decay of diagrams resulting in $DY\bar{Y}X$. If the fraction of Ξ_c producing Λ is the same as that for Λ_c^+, the portion of the branching fraction $B(B\to\Lambda\bar{\Lambda}X)$ from $\Xi_c\bar{Y}X$ intermediate states is just

$$B(B\to\Xi_c\bar{Y}X\to\Lambda\bar{\Lambda}X)=R_{\Xi_c}B^c_{\Lambda_c^+}B^c(\Lambda_c^+\to\Lambda X)\eta\ . \tag{52}$$

Using our values for these quantities this contribution to the $\Lambda\bar{\Lambda}X$ cross section is 0.4%—i.e., all of the $\Lambda\bar{\Lambda}X$ production in B decay would seem to come from $\Xi_c\bar{Y}X$ and we can set a 90%-C.L. limit on $B(B\to DY\bar{Y}X\to\Lambda\bar{\Lambda}X)$ of 0.36%. Given our choice of $\eta=0.75$, this corresponds to a limit of

$$B(B\to DY\bar{Y}X)<0.64\%\ . \tag{53}$$

We note that the decay $\Lambda_c^+\to\Xi^-K^+\pi^+$ has been observed [14]. Values of $B(\Lambda_c^+\to\Xi^-X)$ of order 5% would account for all our observed Ξ^-, eliminating the need for Ξ_c production. Thus our determination of R_{Ξ_c} is somewhat of an upper limit.

VI. CONCLUSIONS

In conclusion, we have made improved measurements of the inclusive yields and momentum distributions of p, Λ, and Ξ^- in B decay. We have also presented convincing, direct evidence for B decay to Λ_c^+. The lack of observation of the $\Lambda\bar{\Lambda}$ and observation of $\Lambda\bar{p}$ correlations suggest that B decays to baryons are dominated by decays of the form $\bar{B}\to\Lambda_c^+\bar{p}X$ and $\bar{B}\to\Lambda_c^+\bar{n}X$. The observation of strong Λl^+ and absence of Λl^- correlations in B-meson decay is consistent with the assumption that all Λ's produced in B-meson decays arise from the secondary decay of charmed baryons. The relative suppression of $\bar{B}\to\Xi^-X$ with respect to $\bar{B}\to\Lambda X$ may be interpreted as evidence that $\bar{B}$ decays to the charmed baryons Ξ_c^+ and Ξ_c^0 must be small. Assuming that the $\bar{B}$ decay to charmed baryons is dominated by the Λ_c^+ charmed baryon and that all light baryons are produced from or in association with it, we have estimated the inclusive branching fractions of B mesons to Λ_c^+ and to n and the inclusive branching fractions of Λ_c^+ to Λ, to p, and to n. In addition we have estimated the exclusive branching fraction $B(\Lambda_c^+\to pK^-\pi^+)=(4.3\pm1.0\pm0.8)\%$. If final

TABLE VI. Summary of quantitative results.

Result	CLEO [2]	ARGUS [3,4]	This paper
	Measured branching fractions and ratios (%)		
$B(B\to pX)$	8.8±0.7±1.0	$8.2\pm0.5^{+1.3}_{-1.0}$	8.0±0.5±0.3
$B(B\to\Lambda X)$	4.2±0.6±0.4	4.2±0.5±0.6	3.8±0.4±0.6
$B(B\to pX)$ (without Λ)		5.5±1.6	5.6±0.6±0.5
$B(B\to\Xi^- X)$		0.28±0.14	0.27±0.05±0.04
$B(\bar{B}\to\Lambda_c^+ X)B(\Lambda_c^+\to pK^-\pi^+)$	0.31±0.05±0.06	0.30±0.12±0.06	0.27±0.05±0.04
$B(B\to\Lambda\bar{\Lambda}X)$		<0.88 (90% C.L.)	<0.5 (90% C.L.)
$f_{\Lambda\bar{\Lambda}}=B(B\to\Lambda\bar{\Lambda}X)/B(B\to\Lambda X)$		<21 (90% C.L.)	<13 (90% C.L.)
$B(B\to p\bar{p}X)$		2.5±0.2±0.2	2.4±0.1±0.4
$f_{p\bar{p}}=B(B\to p\bar{p}X)/B(B\to pX)$		30±3±4	30±2±5
	Results assuming all Λ have Λ_c^+ parentage		
$B(B\to\Lambda\bar{p}X)$		2.3±0.4±0.3	2.9±0.5±0.5
$f_{\Lambda\bar{p}}=B(B\to\Lambda\bar{p}X)/B(B\to\Lambda X)$		54±11±10	76±11±8

states other than $\Lambda_c^+\bar{N}X$ contribute to B decay, this exclusive branching fraction would increase. In Tables VI and VII, we present a numerical summary of our results and compare them with previously published results.

ACKNOWLEDGMENTS

We gratefully acknowledge the effort of the CESR staff in providing the luminosity which made this work possible. P.S.D. thanks the PYI program of the NSF and R. P. thanks the A.P. Sloan foundation for support. This work was supported by the National Science Foundation and the U.S. Department of Energy under Contracts Nos. DE-AC02-76ER01428, DE-AC02-76ER03064, DE-AC02-76ER01545, DE-AC02-78ER05001, DE-AC02-83ER40105, and DE-FG05-86ER40272. The supercomputing resources of the Cornell Theory Center were used in this research.

APPENDIX: MONTE CARLO MODEL OF *B*-MESON DECAYS INTO BARYONS

In this appendix we describe a model of B decays to baryons, which simultaneously reproduces the shape of the $\bar{p}$, Λ, and Λ_c^+ spectra within the limits of the experimental errors. The success of this model further supports the results of our studies on $\Lambda\bar{\Lambda}$, Λ-lepton, and $p\bar{p}$ correlations in B decays, on which we reported in the body of this paper. The salient features of this model are the following.

(a) All decays of $\bar{B}$ mesons to baryons proceed through final states of the form $\Lambda_c^+\bar{N}X$. These states are generated using a Monte Carlo model with a $V-A$ decay matrix element and decays of the form $\bar{B}\to\Pi W^-$; Π is an intermediate particle with mass M_Π, which then decays to $\Lambda_c^+\bar{N}$. The W^- couples to $e^-\bar{\nu}$, $\mu^-\bar{\nu}$, $\tau^-\bar{\nu}$, and $\bar{u}d$ in ratio 12:11:2:75, which is chosen to be consistent with the measured B semileptonic branching fractions. Coupling to the $\bar{c}s$ pair is not allowed kinematically for the range of masses used for Π. The mass of the intermediate Π is chosen according to a Breit-Wigner distribution, whose peak, width, and minimum and maximum mass cutoff values are free parameters of the model. The choice of the Breit-Wigner shape is simply based on convenience and should not be interpreted to have any dynamical content.

(b) All the Λ and p observed in B decays are from the secondary decays of the Λ_c^+ while the $\bar{p}$ are produced in association with it. Only a small fraction of the Λ_c^+ decays has been measured, so we chose a model which reproduces the observed branching fractions into Λ, p, and n, and also agrees with the measured semileptonic branching fraction. The Λ_c^+ branching fractions into

TABLE VII. Estimated branching fractions and ratios (%).

Variable	ARGUS [4] only $\Lambda_c^+\bar{N}X$	This paper only $\Lambda_c^+\bar{N}X$	This paper $\Xi_c\bar{Y}X$ included
	Final states assumed limited to $\Lambda_c^+\bar{N}X$ and $\Xi_c\bar{Y}X$		
$B(\bar{B}\to\Lambda_c^+ X)$		6.4±0.8±0.8	5.1±1.0
$B(B\to nX)$		4.7±1.1±1.2	
$B(B\to nX)$ (without Λ)		3.3±1.1±1.2	
$B(\Lambda_c^+\to pX)$		50±8±14	
$B(\Lambda_c^+\to nX)$		50±8±14	
$B(\Lambda_c^+\to\Lambda X)$		59±10±12	45±15
$B(\Lambda_c^+\to pX)$ (without Λ)		12±10±16	
$B(\Lambda_c^+\to nX)$ (without Λ)		29±9±15	
$B(\Lambda_c^+\to pK^-\pi^+)$	4.1±2.4	4.3±1.0±0.8	5.5±1.7
$B(\bar{B}\to\Xi_c X)/B(\bar{B}\to\Lambda_c^+ X)$			25±12

$\Lambda e^+\nu$, $\Lambda(q\bar{q})e^+\nu$, $\Lambda\mu^+\nu$, $\Lambda(q\bar{q})\mu^+\nu$, $\Lambda(u\bar{d})$, and $\Lambda(q\bar{q})(u\bar{d})$ are selected as 1.8, 1.2, 1.8, 1.2, 32.0, and 22.0 percent, respectively, and add up to 60 percent [40] for the inclusive branching fraction to Λ. The branching fractions to $p(s\bar{u})e^+\nu$, $p(s\bar{u})\mu^+\nu$, $p(s\bar{u})u\bar{d}$, and $p(s\bar{d})$ are selected as 1.0, 1.0, 3.6, and 14.4 percent, respectively, adding up to 20 percent for the inclusive branching fraction to protons without a Λ intermediate state. We chose the inclusive branching fraction to neutrons to be 20 percent with contributions of 1.0, 1.0, and 18.0 percent from the decays $n(s\bar{d})e^+\nu$, $n(s\bar{d})\mu^+\nu$, and $n(s\bar{d})(u\bar{d})$, respectively. The Λ_c^+ semileptonic branching fractions add up to 10 percent in the model [15].

(c) All "$q\bar{q}\rightarrow$hadrons" processes are allowed to proceed according to the Lund prescription [41]. The ratio of popping $s\bar{s}$ relative to $u\bar{u}$ and $d\bar{d}$ is set to 10:45:45.

We simultaneously fit the Λ_c^+, Λ, and $\bar{p}$ momentum spectra obtained from the data by varying the parameters of the Π mass distribution. The best overall fit is obtained when choosing a distribution with peak at 3.35 GeV/c^2, width (FWHM) of 0.50 GeV/c^2, and an allowed mass range from 3.23 to 4.50 GeV/c^2. The minimum mass cutoff is dictated by the rest mass of the $\Lambda_c^+\bar{N}$ combination. In Figs. 2, 4, and 6 we show the Monte Carlo predictions from this model for p, Λ_c^+, and Λ, as smooth curves over the measured momentum spectra. The confidence level of each of these fits is about 23%. Better fits to individual spectra could be obtained by varying the model parameters. Figure 4 also shows Monte Carlo predictions for the Λ_c^+ spectrum for two-, three-, and four-body contributions of the form $\Lambda_c^+\bar{p}m\pi$ ($m=0$, 1, and 2). From the displayed curves it is clear that the decay is dominated by many-body exclusive channels. The latter model predicts an average of three other particles in association with $\Lambda_c^+\bar{N}$.

The Ξ^- spectra may arise due to contributions from $\bar{B}\rightarrow\Lambda_c^+X$ with $\Lambda_c^+\rightarrow\Xi^-X$ and from $\bar{B}\rightarrow\Xi_cX$ with $\Xi_c\rightarrow\Xi^-X$. CLEO has observed [14] the decay $\Lambda_c^+\rightarrow\Xi^-K^+\pi^+$ and has also observed the continuum production of Ξ_c^0 and Ξ_c^+ baryons in the decay modes $\Xi^-\pi^+$ and $\Xi^-\pi^+\pi^+$, respectively [42]. In Fig. 8 the solid curve represents the Monte Carlo prediction from the model $\bar{B}\rightarrow\Lambda_c^+\bar{N}X$ as outlined in the last paragraph, but now with $\Lambda_c^+\rightarrow\Xi^-K^+\pi^+$. All parameters of the Π mass distribution are the same as used for fitting the $\bar{p}$, Λ, and Λ_c^+ spectra. We see that the predicted spectrum from this model is too soft to fit the data. It could be made harder if we choose the decay $\Lambda_c^+\rightarrow\Xi^{*0}K^+$.

We also indicate in Fig. 8 results from a model in which $\bar{B}\rightarrow\Xi_c^0\bar{\Sigma}X$ with $\Xi_c^0\rightarrow\Xi^-X$. In analogy with the model $\bar{B}\rightarrow\Lambda_c^+\bar{N}X$, we introduce an intermediate particle Π, so that $\bar{B}\rightarrow\Pi W^-$ and $\Pi\rightarrow\Xi_c^0\bar{\Sigma}$. The W^- is now allowed to couple to $e^-\bar{\nu}$, $\mu^-\bar{\nu}$, and $\bar{u}d$ in the ratio 12:11:77. The mass of the Π particle again follows a Breit-Wigner distribution, but now with its peak at 4.3 GeV/c^2, a width (FWHM) of 500 MeV/c^2, and an allowed mass range from 3.66 to 5.0 GeV/c^2. These parameters were obtained from fitting the model predictions to the measured Ξ^- momentum spectrum with the branching fractions of Ξ_c^0 into $\Xi^-e^+\nu$, $\Xi^-\mu^+\nu$, and $\Xi^-(u\bar{d})$ fixed at 5, 5, and 90 percent, respectively. The lower Π mass cut now corresponds to the rest mass of the $\Xi_c^0\bar{\Sigma}$ combination. The long dashed curve is the spectrum obtained if the Ξ_c^0 decays to $\Xi^-\pi^+$. If instead the Ξ_c^0 decays to Ξ^-X or to $\Xi^-\pi^+\pi^0$ the momentum spectrum is softer and essentially indistinguishable from the short dashed curve, which is the functional fit as described in the body of the text.

The above Monte Carlo model for B decays to baryons should be considered as an algorithm for reproducing the momentum spectra. The $\bar{p}$, Λ, and Λ_c^+ momentum spectra are reproduced fairly by the above model. The assumption that all baryons are produced from final states of the form $\Lambda_c^+\bar{N}X$ is further supported by Λ-lepton and $\Lambda\bar{\Lambda}$ correlation studies as reported in the body of the paper, lending dynamical support for the model. The Ξ^- spectrum is not reproduced so well, but this may be due to lack of information on all Λ_c^+ decay modes involving Ξ^-. In any case, we can reproduce the Ξ^- spectrum by introducing final states of the form $\Xi_c^0\bar{\Sigma}X$.

[1] CLEO Collaboration, M. S. Alam *et al.*, Phys. Rev. Lett. **51**, 1143 (1983).

[2] CLEO Collaboration, M. S. Alam *et al.*, Phys. Rev. Lett. **59**, 22 (1987).

[3] ARGUS Collaboration, H. Albrecht *et al.*, Z. Phys. C **42**, 519 (1989).

[4] ARGUS Collaboration, H. Albrecht *et al.*, Phys. Lett. B **210**, 263 (1988).

[5] We assume in this article that $\Upsilon(4S)$ decays to $B\bar{B}$ 100% of the time.

[6] D. Andrews *et al.*, Nucl. Instrum. Methods **211**, 47 (1983)—this reference defines the general CLEO detector parameters; D. G. Cassel *et al.*, *ibid.* **A252**, 325 (1986)—this reference details the CLEO 51-layer main drift chamber; C. Bebek *et al.*, Phys. Rev. Lett. **56**, 1893 (1986)—this reference has a description of the 10-layer inner chamber.

[7] CLEO Collaboration, S. Henderson *et al.* (unpublished).

[8] The dE/dx algorithm is actually applied over 90% of 4π, but the resolution is degraded when less than 40 drift chamber cells contribute.

[9] The solid angle coverage of the TOF system is given by $|\cos\theta|<0.57$ and $\Delta\phi=0.88\times2\pi$.

[10] For most momenta the presence of the coil in front of the scintillators makes the TOF of little value in particle identification. However at momenta above 1.0 GeV/c the dE/dx measurements are less efficient than TOF in separating protons.

[11] The inclusive branching fraction $B(B\rightarrow hX)$ for any hadron h from B decay is defined as $B(B\rightarrow hX)=(N_h+N_{\bar{h}})/2N_{B\bar{B}}$, where $\bar{h}$ is the antiparticle of the hadron, N_h and $N_{\bar{h}}$ are the measured numbers of hadrons and antihadrons after correcting for such factors as hadron detection efficiencies, detector geometrical ac-

ceptance, and momentum acceptance. $N_{B\bar{B}}$ is the total number of $B\bar{B}$ meson pairs in the data sample, where both neutral and charged pairs are included. Thus, for example, $B(B\to pX)$ stands for $B(B\to pX)+B(B\to\bar{p}X)$ as averaged over charged and neutral B mesons and over B and $\bar{B}$ mesons. Consistent with this, unless specified in the text, any reference to a particle or to its decay mode implicitly applies to the charge-conjugate states as well.

[12] The functions were of the form

$$f(x)=\frac{Ag(x)}{\int_0^{x_{\max}} g(x)dx},$$

$$g(x)=x^n(x_{\max}-x)^m(1+ax+bx^2),$$

in which the parameter A is the product of the area and the bin size of the momentum distribution. For an individual fitting attempt, n, m, and $x_{\max}$ were fixed and A, a, and b determined by the fit. Wide ranges of the powers n and m and of the cutoff $x_{\max}$ were tried; the fitted value of A is not sensitive to the choice of these three parameters, so a typical fit was used to determine the mean yield and its statistical uncertainty. For a conservative estimate of the systematic uncertainty of this procedure the range of values of the yield is used.

[13] An alternative procedure for $\bar{p}$ and Λ would be to use either the Monte Carlo model as described in the Appendix or simple functional forms to determine what fraction of baryons lie within the tabulated momentum interval and then divide the observed yield by this acceptance. This procedure leads to larger statistical uncertainties than if one fits the entire spectrum, since some of the momentum bins have small numbers of events. The acceptance correction for p and $\bar{p}$ is $(90\pm5)\%$, giving $39\,131\pm2790\pm2247$ p's and $\bar{p}$'s actually produced. For Λ the acceptance factor is $(85\pm10)\%$, giving $18\,764\pm2153\pm2735$ Λ's actually produced.

[14] CLEO Collaboration, P. Avery *et al.*, Phys. Rev. D **43**, 3599 (1991).

[15] Particle Data Group, J. J. Hernández *et al.*, Phys. Lett. B **239**, 1 (1990).

[16] G. C. Fox and S. Wolfram, Phys. Rev. Lett. **41**, 1581 (1978). The parameter R_2 is the ratio of H_2 to H_0.

[17] B. Gittelman and S. Stone, in *High Energy Electron-Positron Physics,* edited by A. Ali and P. Soding (World Scientific, Singapore, 1987), pp. 275–359.

[18] P. Avery, in *Linear Collider BB Factory,* Proceedings of the Workshop, Los Angeles, California, 1987, edited by D. Stock (World Scientific, Singapore, 1987).

[19] CLEO Collaboration, R. Fulton *et al.*, Phys. Rev. Lett. **64**, 16 (1990).

[20] ARGUS Collaboration, H. Albrecht *et al.*, Phys. Lett. B **234**, 409 (1990).

[21] CLEO Collaboration, P. Avery *et al.*, Phys. Lett. B **223**, 470 (1989).

[22] If, for example, the hyperon Y was to have equal probability of manifesting itself as Λ, Σ^-, Σ^0, and Σ^+, then $f_{\Lambda\bar{\Lambda}}$ would have a value of 0.25 if $DY\bar{Y}X$ were dominant.

[23] DELCO Collaboration, W. Bacino *et al.*, Phys. Rev. Lett. **43**, 1073 (1979).

[24] ARGUS Collaboration, H. Albrecht *et al.*, Phys. Lett. B **192**, 245 (1987).

[25] CLEO Collaboration, M. Artuso *et al.*, Phys. Rev. Lett. **62**, 2233 (1989). This reference details the technique and gives our more preliminary value of the mixing parameter of $r=0.19\pm0.06\pm0.06$.

[26] CLEO Collaboration, R. Fulton *et al.*, Phys. Rev. D **43**, 651 (1991). We use the CLEO measurement of the mixing parameter in computing this correction. The value of $r=0.165\pm0.065$ was derived under the assumption that neutral and charged $B\bar{B}$ pairs are equally produced and that the lifetimes of neutral and charged B's are the same.

[27] If in Eq. (12) we had assumed that $\Lambda\bar{\Lambda}$ type of final states would be the source of *all* observed Λ, then the final measured Λl^- correlation signal would be 14.7 ± 9.6.

[28] The requirements for a p or $\bar{p}$ to be "strongly identified" are the same as in our analysis of $B(\bar{B}\to pX)$.

[29] The breakdown of observed events in the four relevant channels is 856 ± 82 $\Lambda\bar{p}$, 670 ± 89 $\bar{\Lambda}p$, 115 ± 60 Λp, and 75 ± 33 $\bar{\Lambda}\bar{p}$.

[30] Jonathan D. Lewis, Ph.D. thesis, Cornell University, 1990.

[31] Mark III Collaboration, J. Adler *et al.*, Phys. Lett. B **208**, 152 (1988); Mark III Collaboration, J. Adler *et al.*, Phys. Rev. Lett. **60**, 89 (1988).

[32] We have also done detailed analysis of these observations, taking the mean of $B\bar{B}$ backgrounds to be 2.7 with Gaussian standard deviation of 1.0 and the mean from the continuum to be distributed according to the Poisson law xe^{-x}. This mean from the continuum is then scaled by 2.08 to account for the larger luminosity collected at the $\Upsilon(4S)$. If we then ask what signal from $D^{*+}p\bar{p}X$ would have given us 4 or more events 90% of the time, the limit is 1.5 events. On the other hand, if we follow the Particle Data Group formulation for obtaining a *conservative* 90% limit, we should have used 3.6 events.

[33] This is strictly true if we ignore the small energy penalty paid for creating a $u\bar{d}$ pair needed in some of the diagrams. Note also that we have ignored contributions from higher-mass charmed mesons.

[34] Since the decay $B\to\Lambda_c^+X$ and its charge conjugate are not possible, $B_{\Lambda_c^+}$ actually stands for $B(\bar{B}\to\Lambda_c^+X)+B(B\to\overline{\Lambda_c^+}X)$ as averaged over charged and neutral B mesons.

[35] I. Bigi, Phys. Lett. **106B**, 510 (1981).

[36] LEBC-EHS Collaboration, M. Aguilar-Benitez *et al.*, Phys. Lett. B **199**, 462 (1987). This reference gives a lower limit of 4.4% (90% C.L.), which was changed to the value given in the text by S. Gentile, in *Current Issues in Hadron Physics,* Proceedings of the XXIIIrd Rencontre de Moriond, Les Arcs, France, 1988, edited by J. Tran Thanh Van (Editions Frontières, Gif-sur-Yvette, 1989).

[37] Mark II Collaboration, G. Abrams *et al.*, Phys. Rev. Lett. **44**, 10 (1980).

[38] The Ξ_c stands for the sum of Ξ_c^+ and Ξ_c^0.

[39] Here we assume Ξ^-p correlations are similar to Λp correlations and that the exclusive branching fractions for Ξ_c to Λ and to p are the same as those for Λ_c^+. The branching fraction $B(\Lambda_c^+\to\Lambda X)$ is particularly affected by including final states of the form $\Xi_c\bar{\Lambda}X$ since these final states directly subtract from the total number of Λ that are products of Λ_c^+ decay.

[40] Varying this value by up to 10% makes no appreciable difference in the fits to the various spectra.

[41] B. Anderson *et al.*, Phys. Rep. **91**, 33 (1983).

[42] CLEO Collaboration, M. S. Alam *et al.*, Phys. Lett. B **226**, 401 (1989).